EITN90 Radar and Remote Sensing
Lecture 12: An overview of radar imaging

Daniel Sjöberg

Department of Electrical and Information Technology

Learning outcomes of this lecture

In this lecture we will

- See how images can be formed from radar signals collected at different locations.
- Learn what determines the achievable resolution of the image.
- See the basics of a few imaging algorithms.
- Observe typical phenomena in radar images.

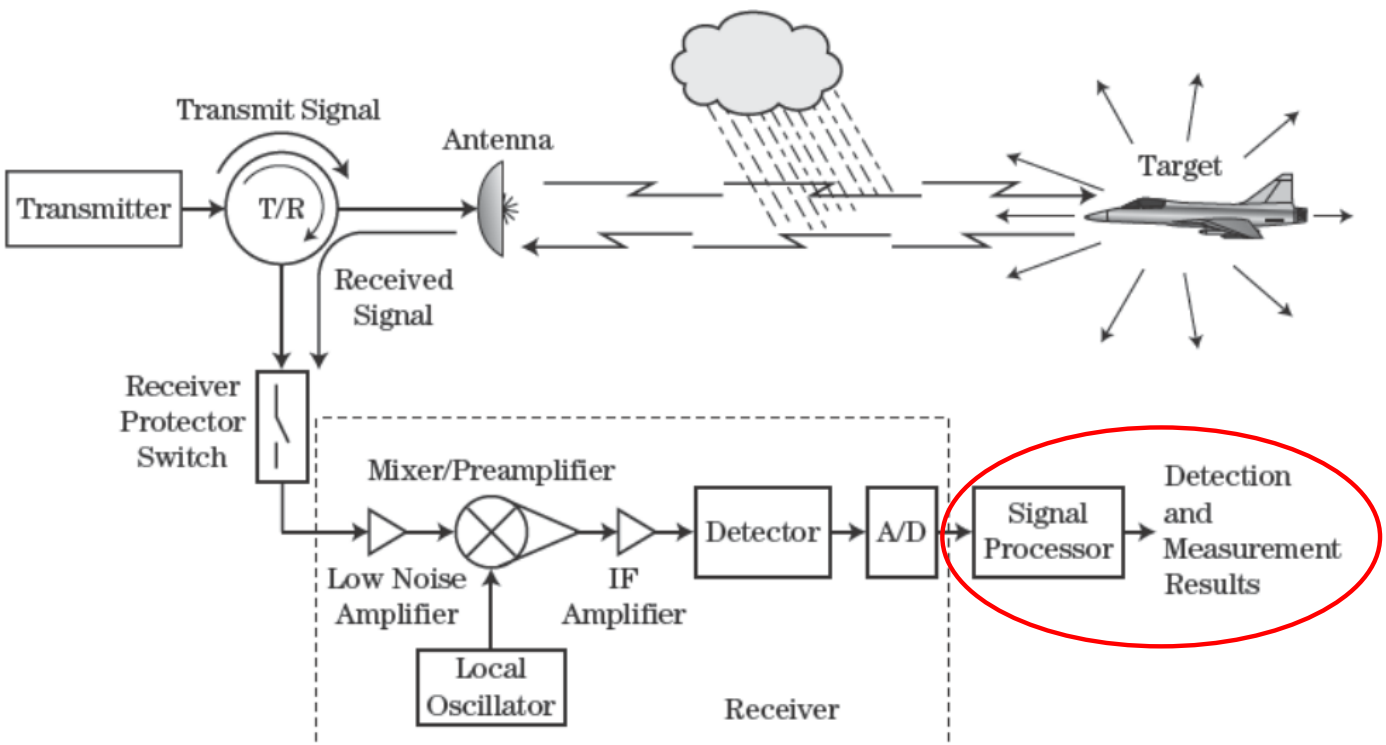

FIGURE 1-1 ■ Major elements of the radar transmission/ reception process.

Outline

Outline

Radar vs optical photo

FIGURE 21-1 ■
Two renderings of Albuquerque Airport. (a) Synthetic Aperture Radar image, and (b) optical overhead photograph. (Images courtesy of Sandia National Laboratories.)

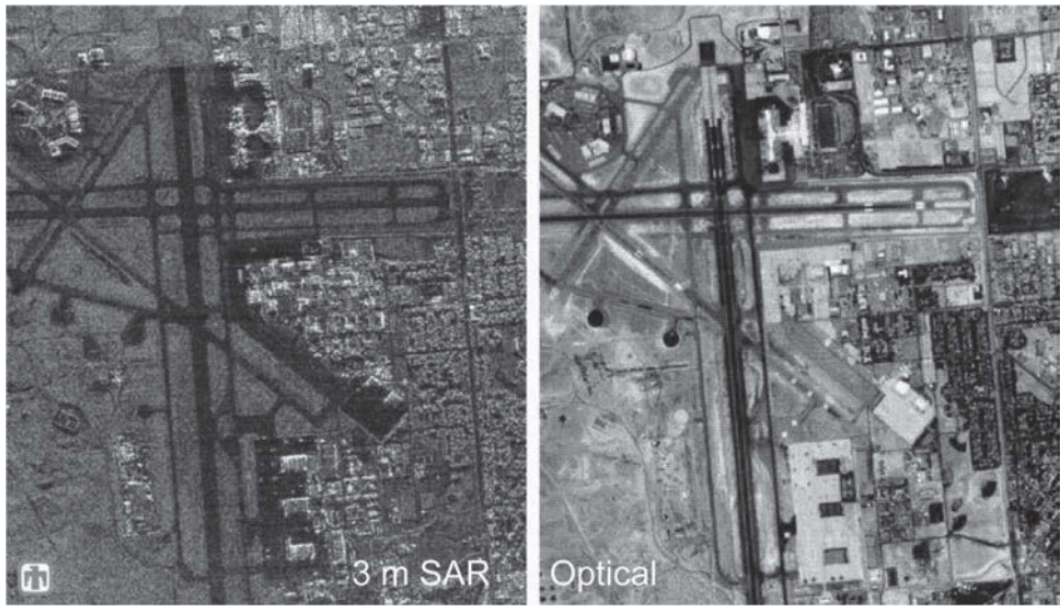

(a) (b)

Some benefits of radar (cost of providing its own illumination, long measurement time, computationally demanding):

- Weather tolerant.
- Emphasizes man-made objects.
- Provides fine resolution at large range.
- Can penetrate foliage and other obstacles.
- Requires coherent operation.
- Polarization may provide additional information.

Synthetic Aperture Radar (SAR)

SAR can be thought of in at least three different aspects:

- SAR as a large synthetic antenna aperture.
- SAR as range-Doppler imaging.
- SAR as a signal processing exercise.

SAR as a large synthetic antenna aperture

FIGURE 21-2 ■
Overhead view illustrates radar platform moving from left to right with side-looking antenna having main beam and ground footprint pointed towards the top.

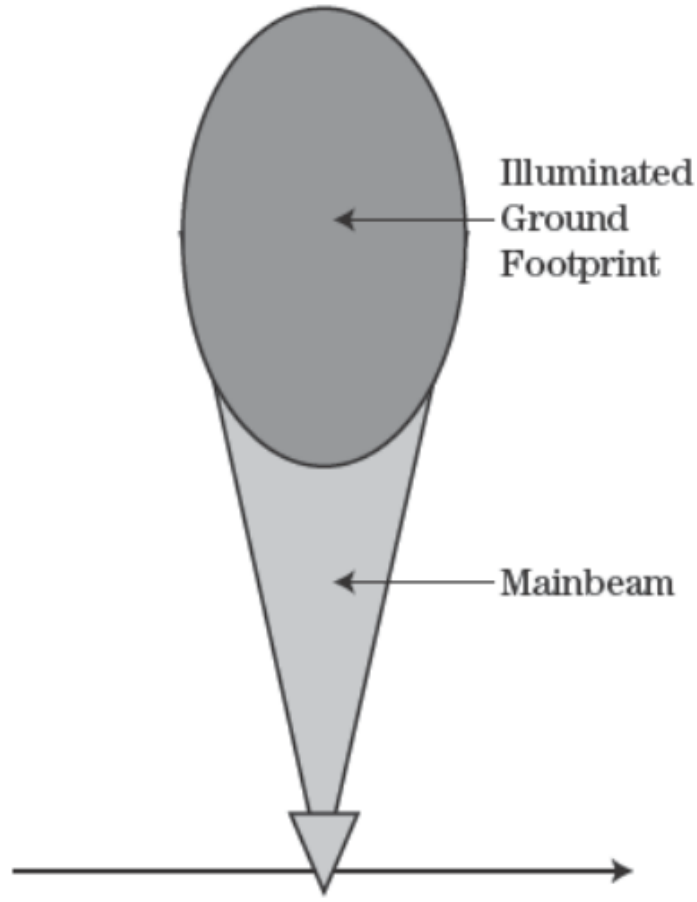

The cross-range resolution can be seen as the effective beam width of an antenna with

$$\Delta \mathrm{CR} \approx R\theta_3 \approx R\frac{\lambda}{2D_{\mathrm{SAR}}}$$

SAR as range-Doppler imaging

FIGURE 21-3 ■
Coordinate system showing azimuth, elevation, and cone angles, and vectors for platform velocity and direction to target.

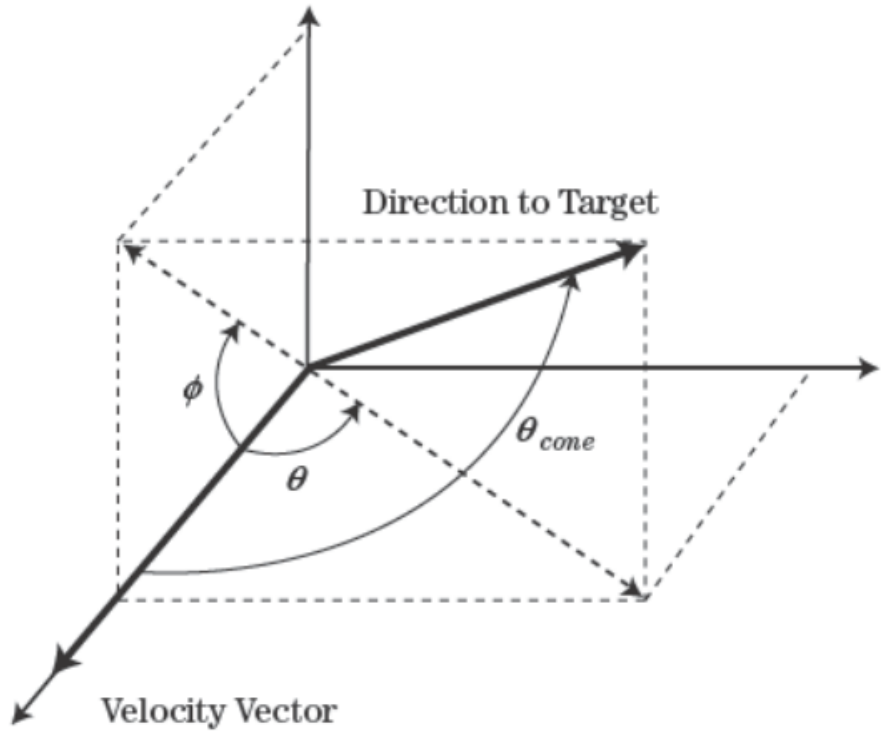

The platform is moving in a certain direction relative to the scene, causing a Doppler shift $f_\mathrm{d} = 2v\cos\theta_\mathrm{cone}/\lambda$ in the received signal.

$$\Delta\mathrm{CR} = R\Delta\theta = R\frac{\lambda\Delta f_\mathrm{d}}{2v\sin\theta} = R\frac{\lambda}{2vT_\mathrm{d}\sin\theta} = R\frac{\lambda}{2D_\mathrm{SAR}\sin\theta}$$

In the book, the broadside angle $\theta_\mathrm{b} = \theta + 90°$ is used, resulting in $\sin\theta \to \cos\theta_\mathrm{b}$.

SAR as a signal processing exercise

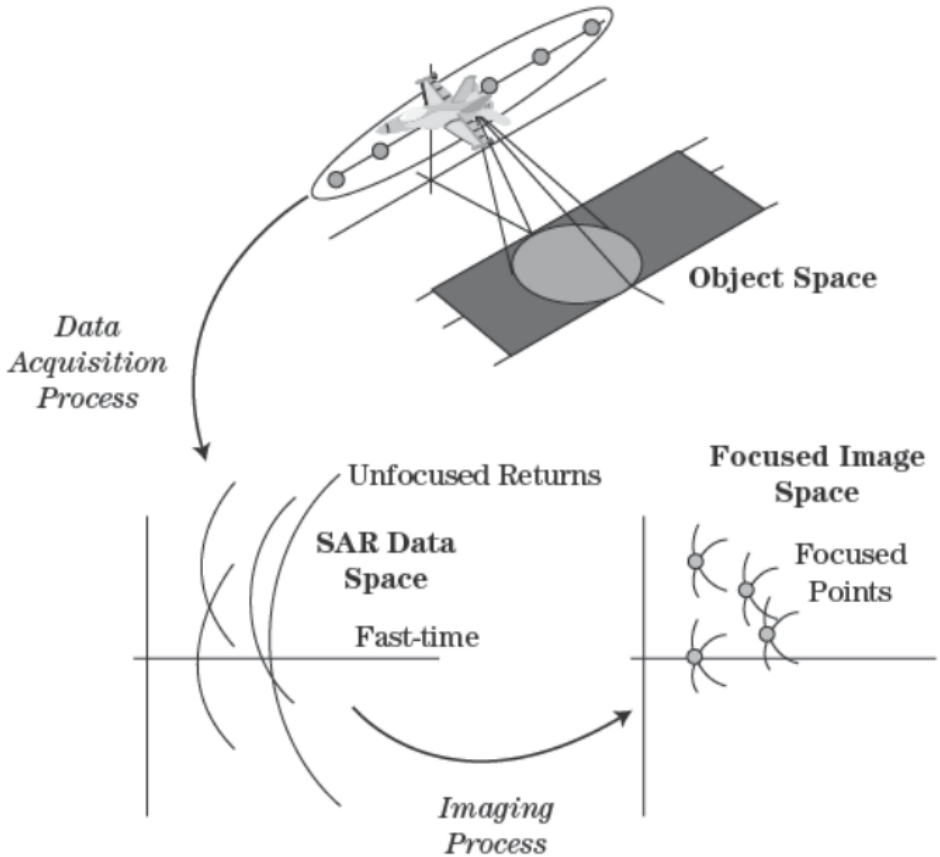

FIGURE 21-5 ■ The SAR process involves three spaces and two transformations. Data acquisition provides the transformation from scene reflectivity to raw data, while image formation operates on the raw data to yield the final SAR image.

The image is the result of the relation between three data spaces:

- Object space, defined by the scatterers.
- Data space, the raw radar measurements.
- Image space, the final synthetic image.

Down-range and cross-range coordinates

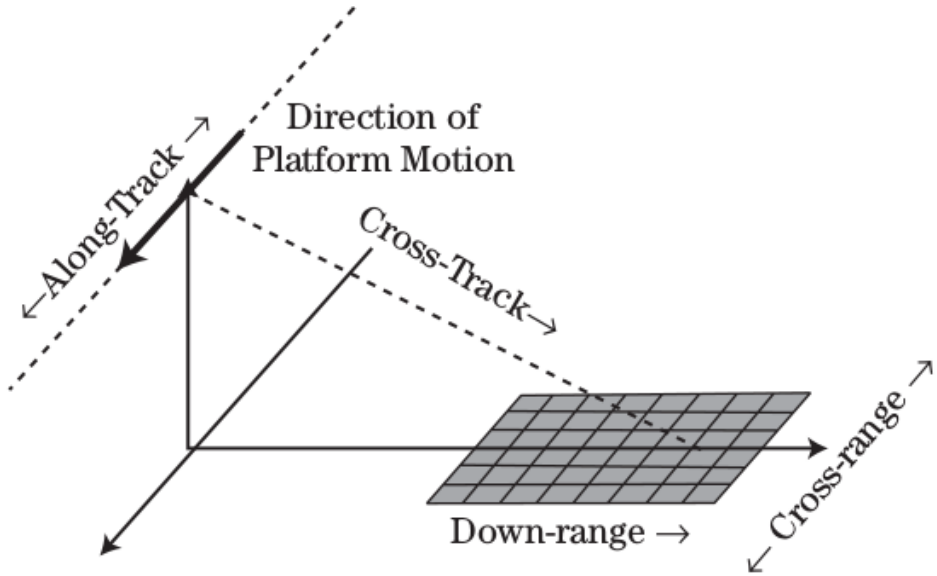

FIGURE 21-4 ■ Location in a SAR image is usually defined as a function of along-track and cross-track coordinates, or down-range and cross-range coordinates. For side-looking collections these coordinate systems are nearly equivalent.

- The down-range coordinate corresponds to fast time (delay for individual pulses).
- The cross-range coordinate corresponds to slow time (phase difference between pulses).

Outline

Down-range and cross-range resolutions

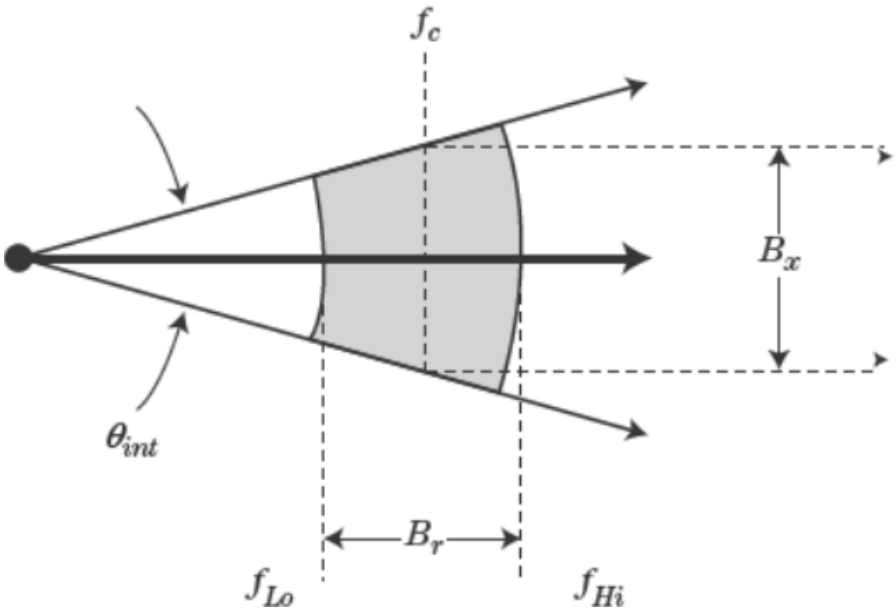

FIGURE 21-6 ■ Data support for a SAR collection is two dimensional and is a function of the waveform frequencies and integration angle. These quantities may be depicted in a polar coordinate system.

The resolutions in down-range and cross-range can be written

$$\Delta R = \frac{c}{2B_{\mathrm{r}}}$$

$$\Delta \mathrm{CR} = \frac{c}{2B_x} = \frac{c}{2f_{\mathrm{c}}\theta_{\mathrm{int}}} = \frac{R\lambda_{\mathrm{c}}}{2D_{\mathrm{SAR}}}$$

Different waveforms

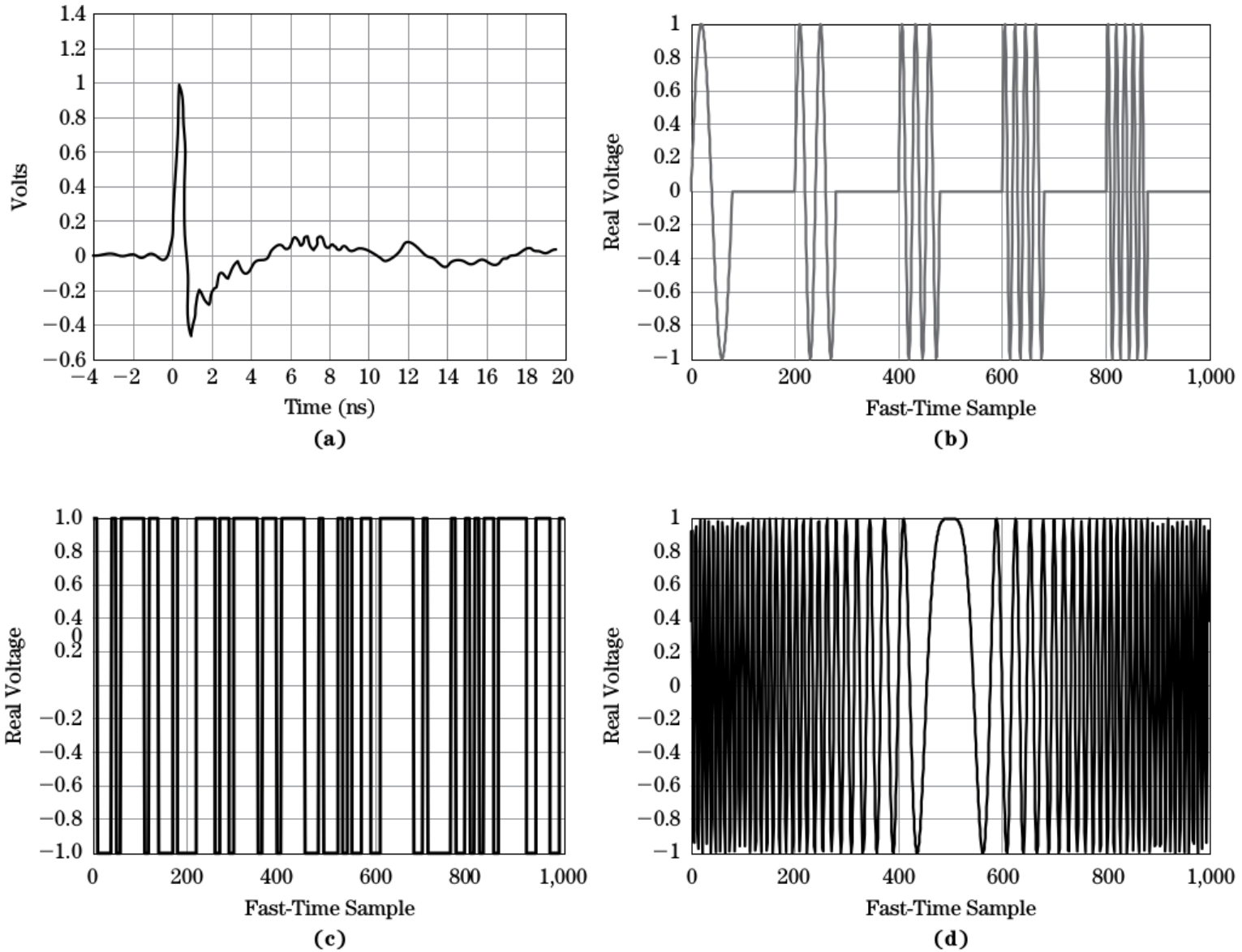

FIGURE 21-7 ■ Four options for wideband waveforms are (a) a short-time pulse, (b) a stepped-frequency series of pulses, (c) a bi-phase modulated pulse, or (d) a linear FM pulse.

Illumination options for data collection

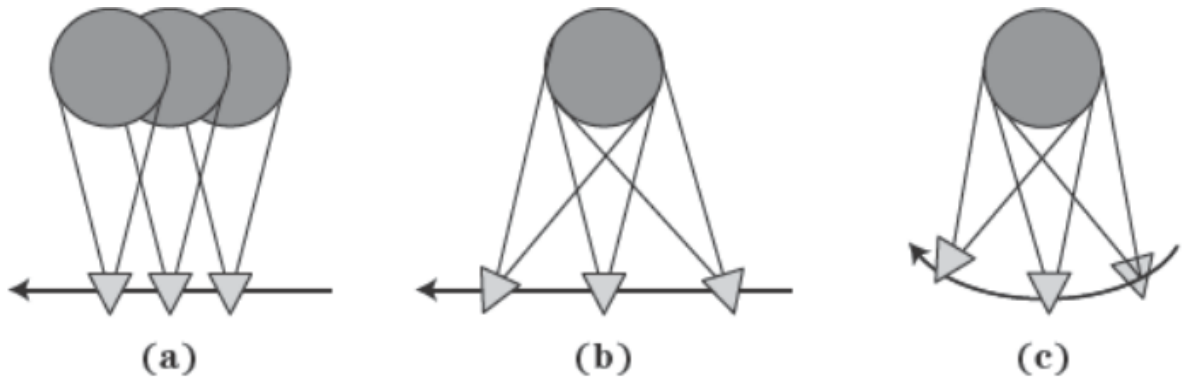

FIGURE 21-8 ■ Three collection options for achieving integration angle are (a) stripmap, (b) spotlight with mechanical or electronic steering of the real antenna beam onto a scene of interest, or (c) spotlight realized by flying a circle about the scene of interest.

Both the flightpath and the direction of the antenna can affect the total illumination of the scene.

Integration angle

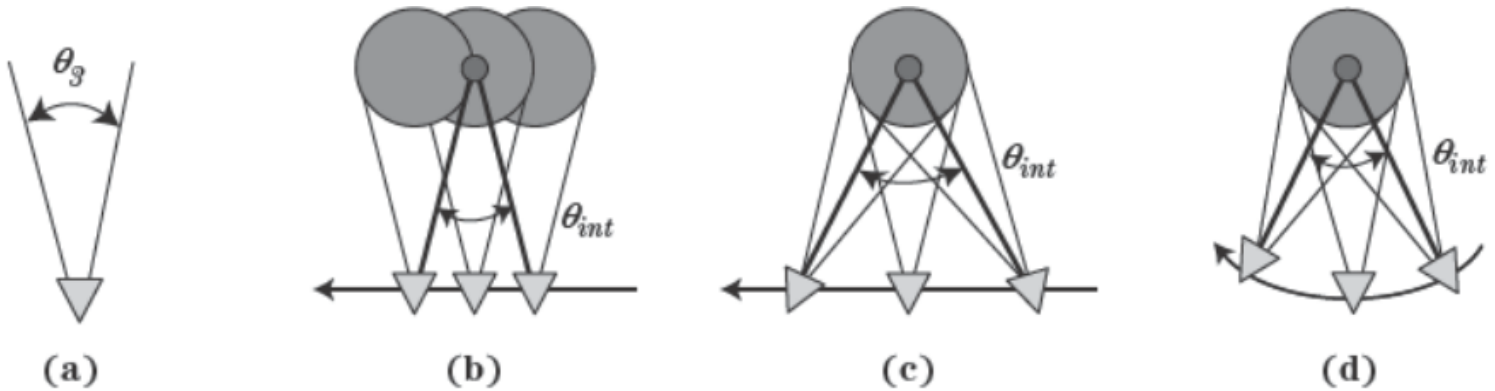

FIGURE 21-9 ■ Given the beamwidth of a real antenna (a), the stripmap integration angle (b) is limited by the real beamwidth, while spotlighting with linear (c) or circular (d) flight paths can realize integration angles greatly exceeding the real antenna beamwidth.

In the stripmap approach, θ_{int} is limited by the real antenna beam. Spotlight scenarios can greatly improve the integration angle.

The linear path and the circular path give very different signal histories, giving rise to different algorithms.

Cross-range sampling requirement

When using sampling distance d, the phase change between two samples is

$$\Delta\psi = 2\pi\left(\frac{2\delta R}{\lambda}\right) = 4\pi\frac{d\sin(\theta_3/2)}{\lambda}$$

To keep the successive phase changes $|\Delta\psi| < \pi$ requires

$$d < \frac{\lambda}{4\sin(\theta_3/2)} \approx \frac{\lambda}{2\theta_3} \approx \frac{\Delta\mathrm{CR}}{2}$$

For wideband pulses, use the minimum wavelength $\lambda_{\min}$.

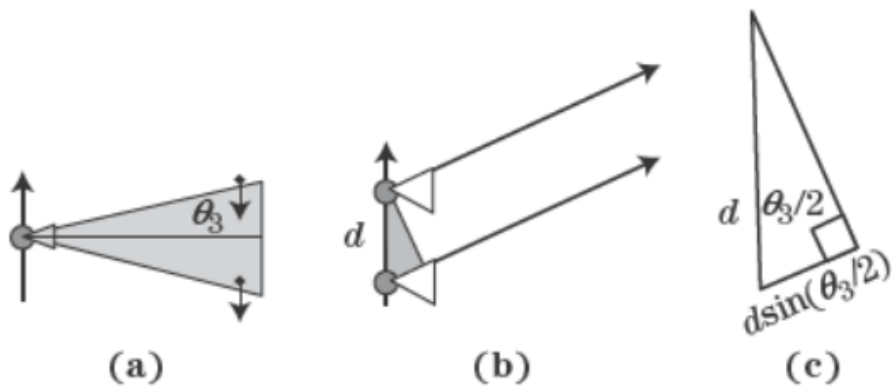

FIGURE 21-10 ■ Geometry for deriving the along-track sampling requirements for stripmap mode, (a) platform moving from bottom to top with antenna pointed to the right, (b) distance between along-track sample points d, and (c) differential range change to a scatterer on the leading edge of the mainbeam.

Outline

Radar vs camera

FIGURE 21-11 ■ Geometry of overhead photography of a scene of interest as compared to a typical SAR collection.

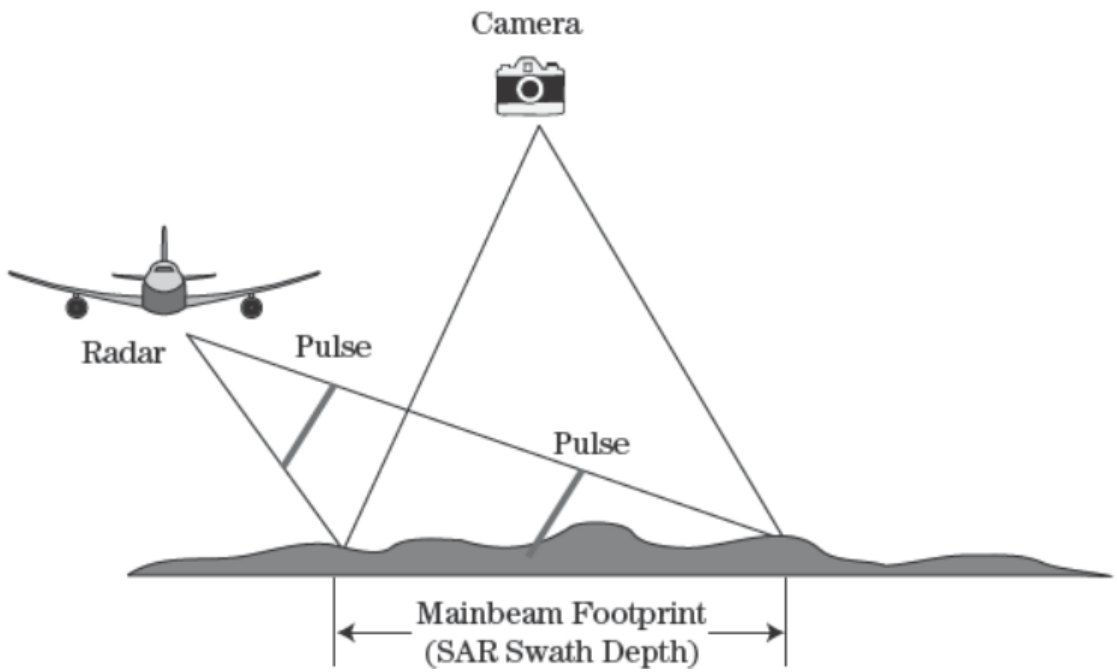

A radar sensor is typically side-looking instead of overhead-looking.

▸ Discussion

Radar vs camera

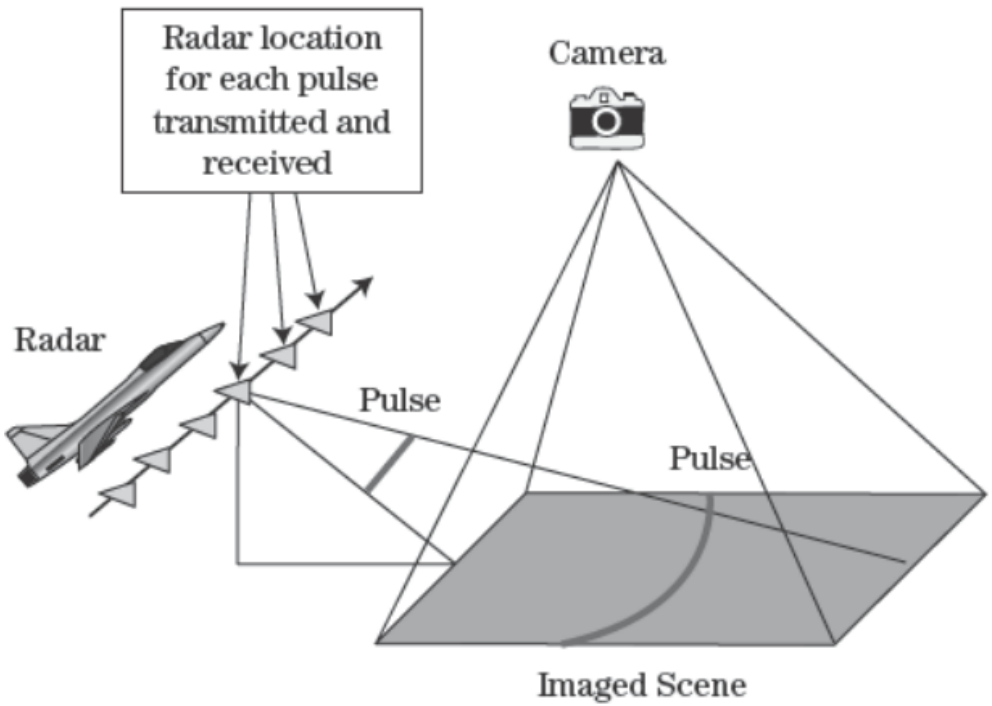

FIGURE 21-12 ■ The camera generates a 2-D image in one take, whereas the radar must collect data pulse-by-pulse over a long dwell.

A radar sensor collects data pulse-by-pulse instead of 2D image-by-2D image. Note the radar provides its own illumination.

Stop-and-hop model

FIGURE 21-13 ■ Every pulse illuminates the entire scene of interest and produces a 1-D, complex range profile.

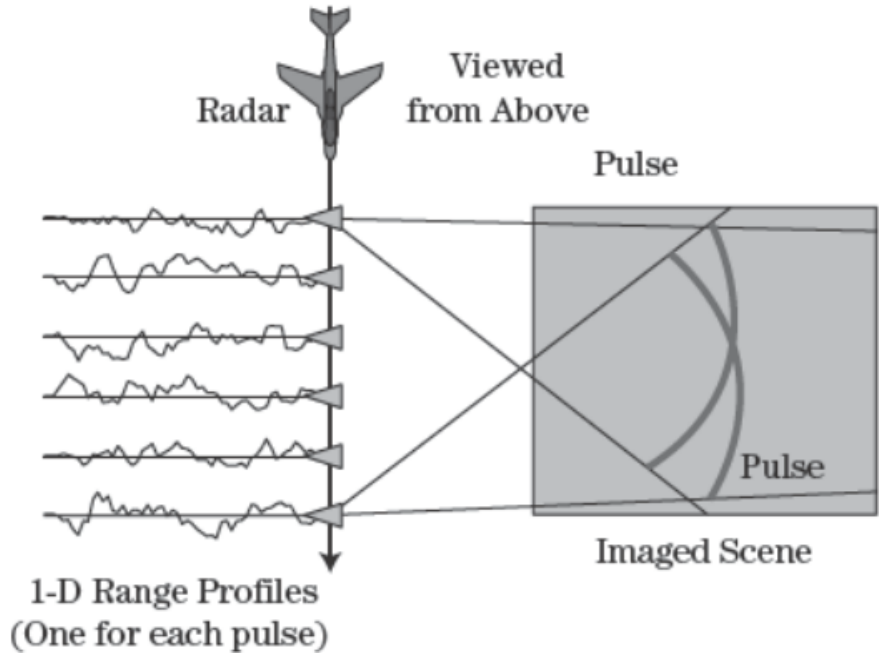

A stream of I/Q data is recorded (phase is important). The radar is moving continuously, but each signal is considered to be recorded in a stationary frame.

Cross-range phase changes

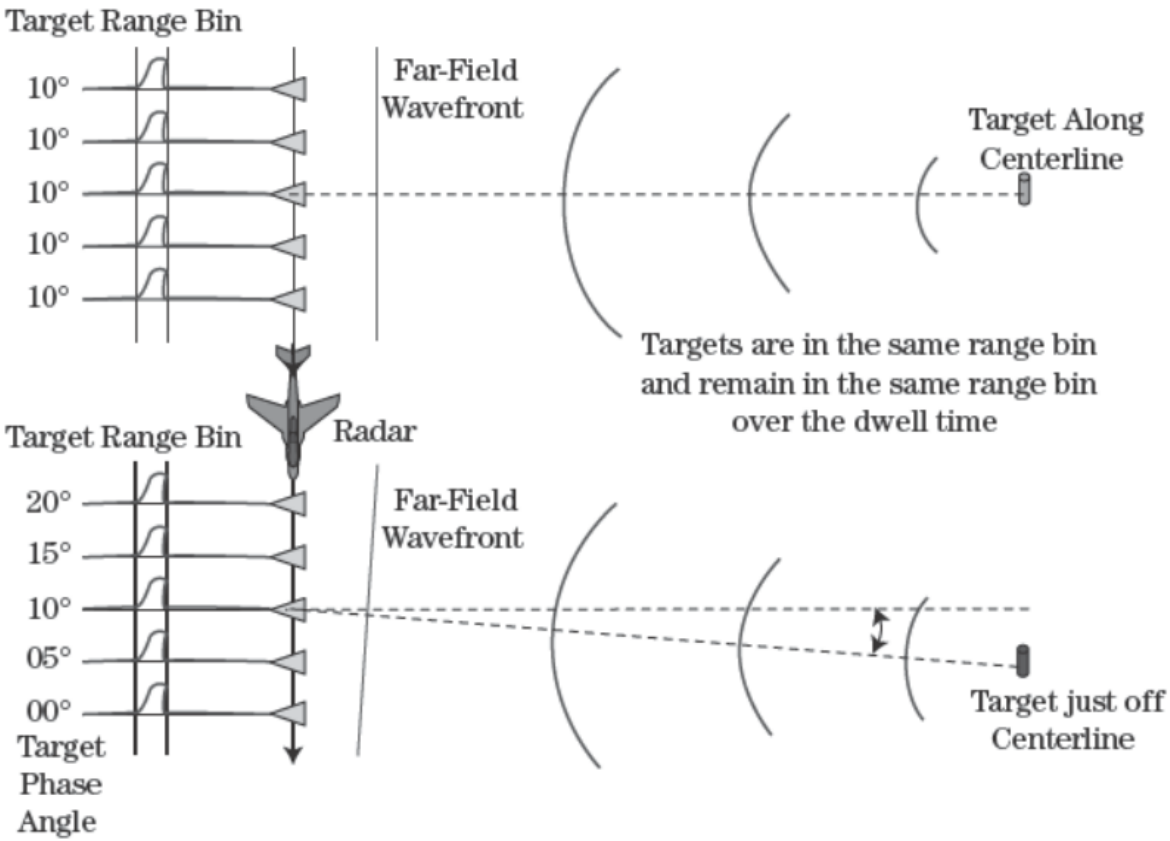

FIGURE 21-14 ■ Small changes in the cross-range location of a scatter cause a negligible change in the apparent range bin for that return but a significant change in the induced pulse-to-pulse phase progression for that return.

A target off the centerline causes phase changes in cross-range, corresponding to the Doppler shift. The target may still be in one single range bin.

Outline

Stripmap coordinates

FIGURE 21-15 ■
The SAR process as depicted in Figure 21-5 with axes defined.

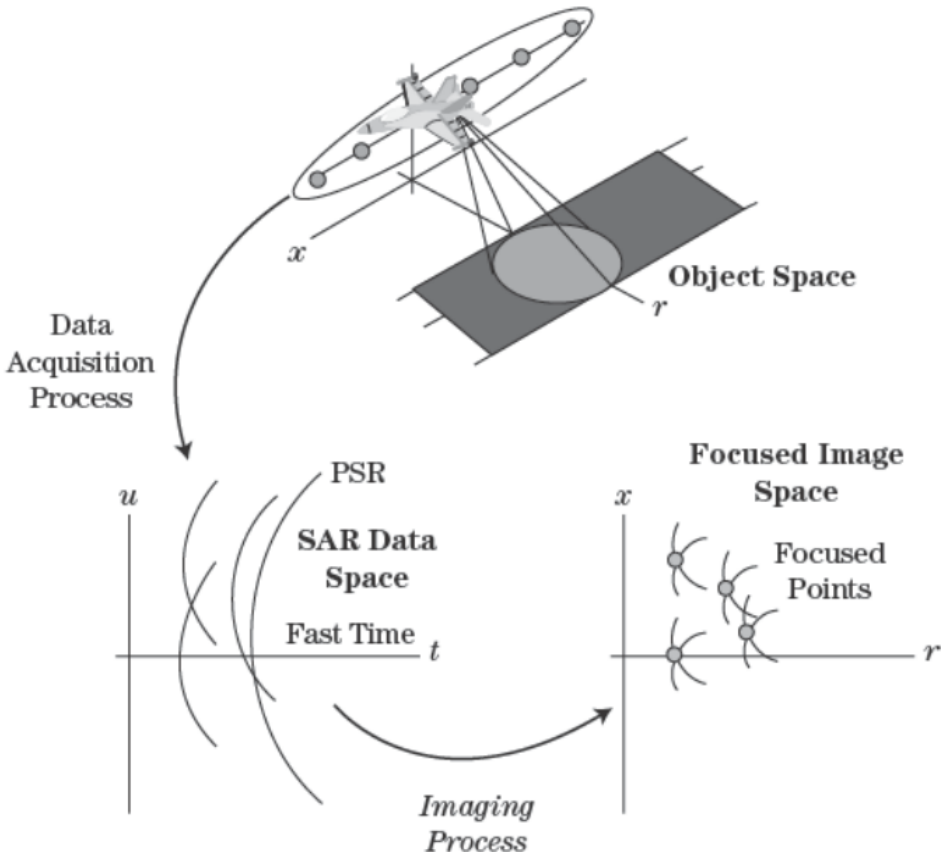

- Platform moves linearly, parameterized by position u.
- Complex reflectivity $g(x, r)$.
- Complex data $d(u, r)$.
- Complex image $f(x, r)$.

Slant range

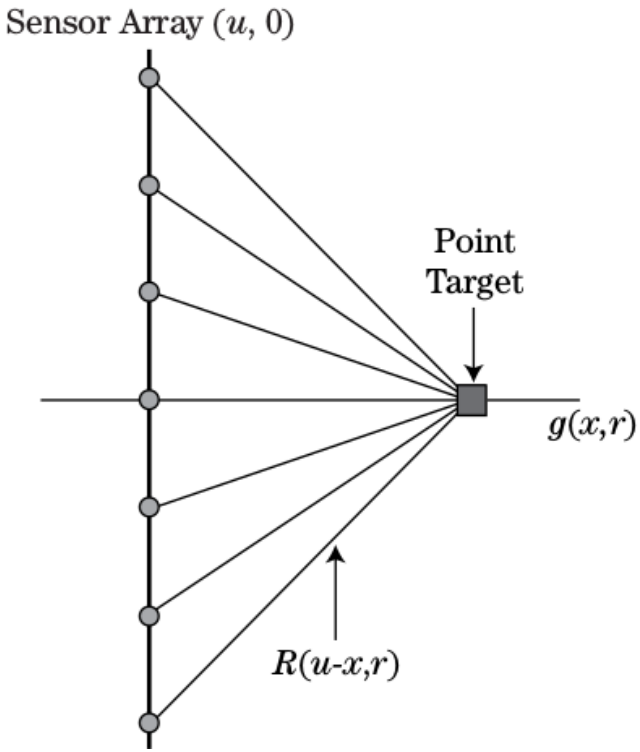

FIGURE 21-16 ■
Variation in slant range to a scatter at (x, r) due to platform motion.

The slant range $R(u; x, r)$ is given by

$$R(u; x, r) = \sqrt{(u - x)^2 + r^2} \quad \Rightarrow \quad t(u; x, r) = \frac{2}{c}\sqrt{(u - x)^2 + r^2}$$

The translational invariance from the dependence on $u - x$ enables us to consider the generic response at $x = 0$.

Point spread response (PSR)

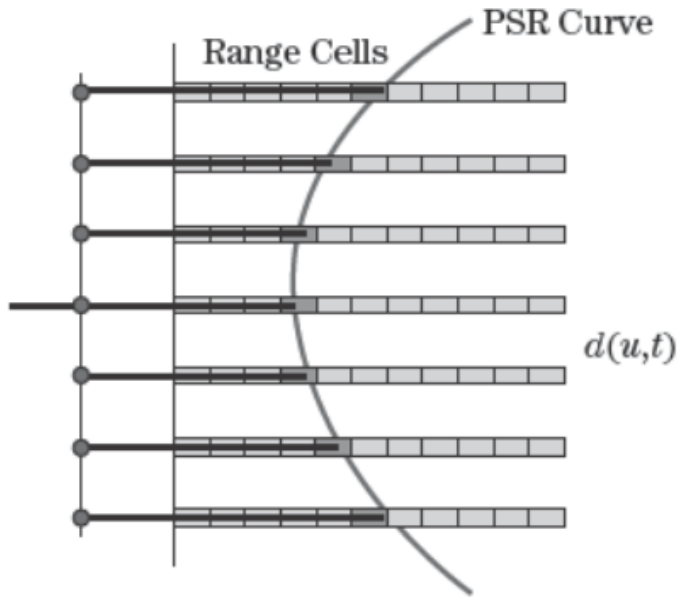

FIGURE 21-17 ■ The range variation to the scatterer over the dwell is described by the PSR. The PSR is manifested in the raw data as a hyperbolic migration of the return from a scatterer across compressed range bins.

The point spread response $t(u; x, r) = \frac{2}{c}\sqrt{(u-x)^2 + r^2}$ describes a hyperbola in the data domain $d(u, t)$, with a vertex depending on (x, r).

Dependence of PSR on down-range

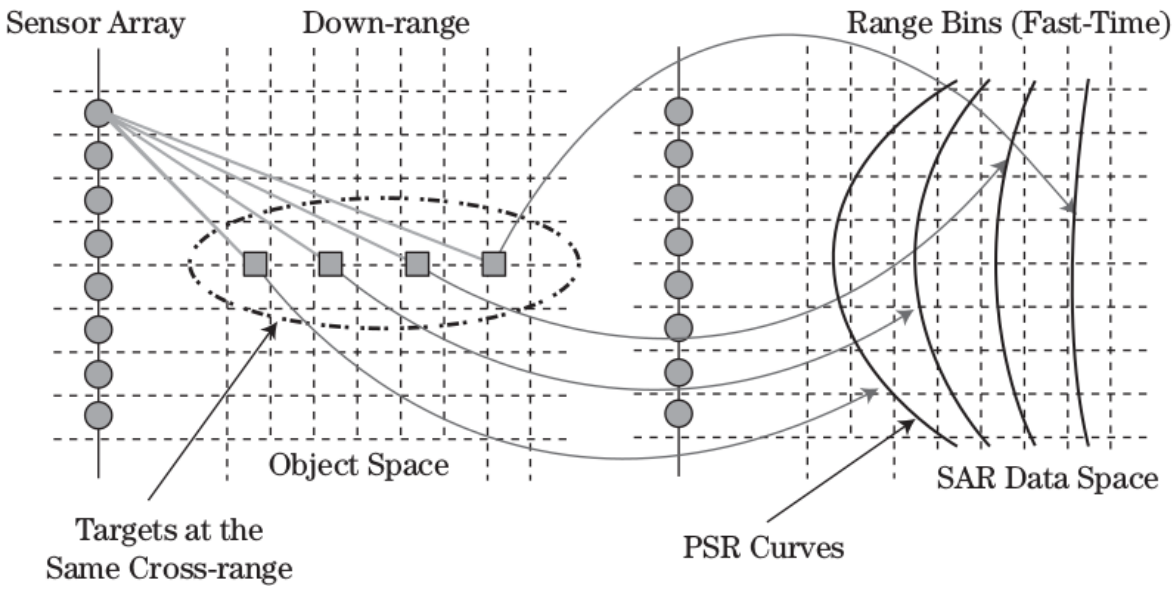

FIGURE 21-18 ■ Scatterers at different cross-track (down-range) locations have different PSR forms. Curvature decreases as range increases.

The PSR is not a simple translation when considered as a function of down-range r:

$$t(u; r+\Delta r) = \frac{2}{c}\sqrt{u^2 + (r+\Delta r)^2} = \frac{2}{c}\sqrt{u^2 + r^2 + 2r\Delta r + (\Delta r)^2}$$
$$\neq t(u; r) + \frac{2}{c}\Delta r$$

More bowing of the PSR for scatterers with close range.

Variations of PSR in cross-range and down-range

FIGURE 21-19 ■
Scatterers at different along-track (cross-range) location have the same PSR form, but with an along-track offset.

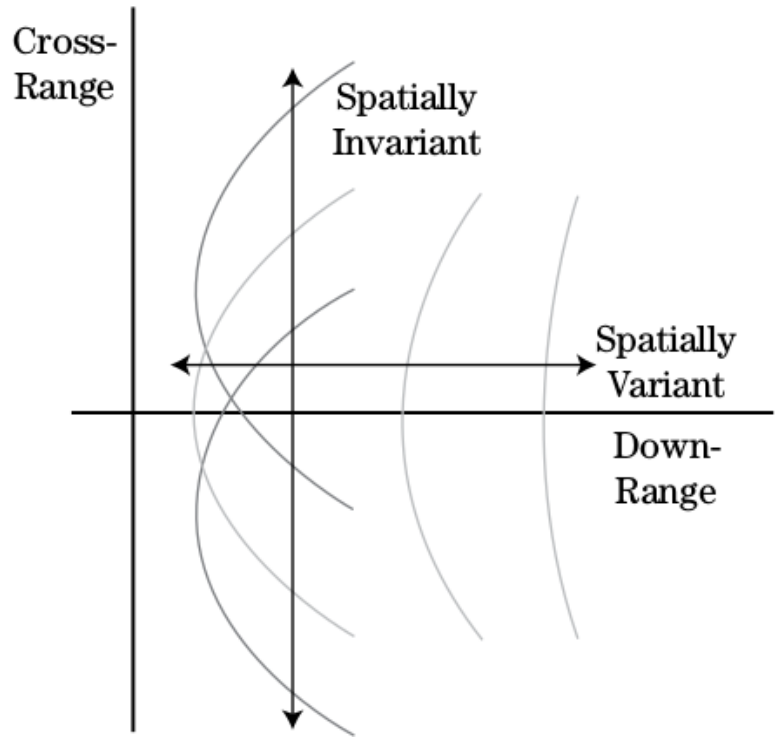

The shape invariance in cross-range (along-track) can be used for image formation.

Range-Doppler data

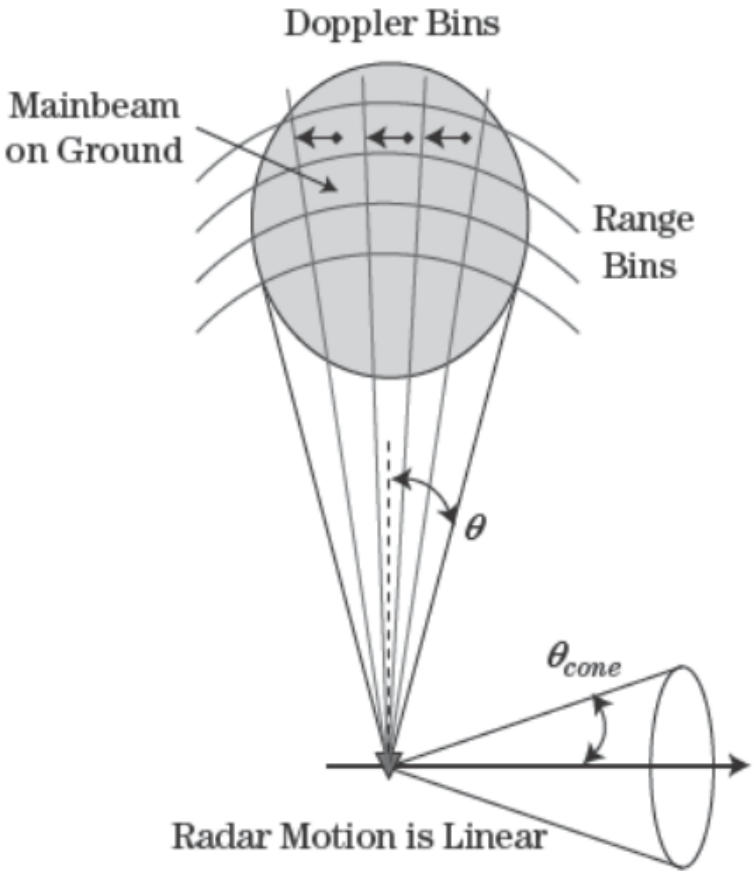

FIGURE 21-20 ■ Arranging ground returns as a function of slant range and Doppler yields a 2-D rendering of the scene of interest.

Range bins are formed as functions of fast time, and Doppler bins are formed as functions of slow time (phase shifts between pulses) due to Doppler shift

$$f_{\mathrm{d}} = \frac{2v}{\lambda} \sin\theta$$

Short dwell time compared to range

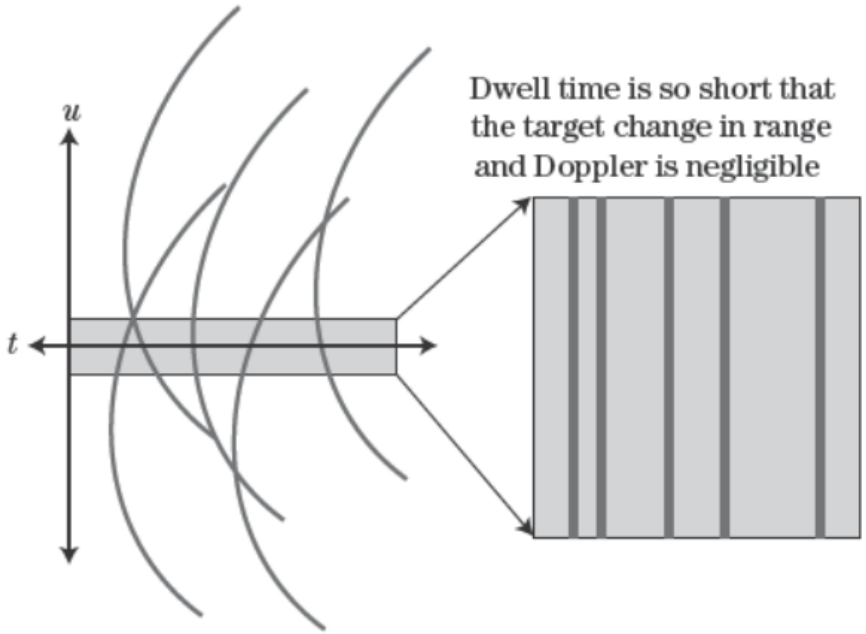

FIGURE 21-21 ■
For short collection times and coarse range bins each hyperbolic PSR is constrained to one range bin over the dwell.

At long range, the PSR splits into two terms:

$$t(u;x,r) = \frac{2}{c}\sqrt{(u-x)^2+r^2} = \frac{2r}{c}\sqrt{1+\frac{(u-x)^2}{r^2}}$$

$$\approx \frac{2r}{c}\left(1+\frac{1}{2}\frac{(u-x)^2}{r^2}\right) = \frac{2}{c}\left(r+\frac{u^2}{2r}-\frac{ux}{r}+\frac{x^2}{2r}\right)$$

$$= \frac{2}{c}\left(r+\frac{x^2}{2r}\right)+\frac{2}{c}\left(\frac{u^2}{2r}-\frac{ux}{r}\right) = t_0(x,r)+\Delta t(u;x,r)$$

Cross-range position as spatial frequency

Assuming the u^2 term can be ignored (requires $D_{\mathrm{SAR}} < \sqrt{r\lambda_c}$)

$$\Delta\psi = 2\pi f_c \Delta t(u; x, r) = \frac{4\pi}{\lambda_c}\left(\frac{u^2}{2r} - \frac{ux}{r}\right) \approx -u\frac{4\pi}{\lambda_c}\frac{x}{r}$$

shows that the **phase change is linear as a function of platform position** u. The spatial frequency is proportional to x:

$$k_u = \frac{\partial}{\partial u}\Delta\psi = -\frac{4\pi}{\lambda_c}\frac{x}{r}$$

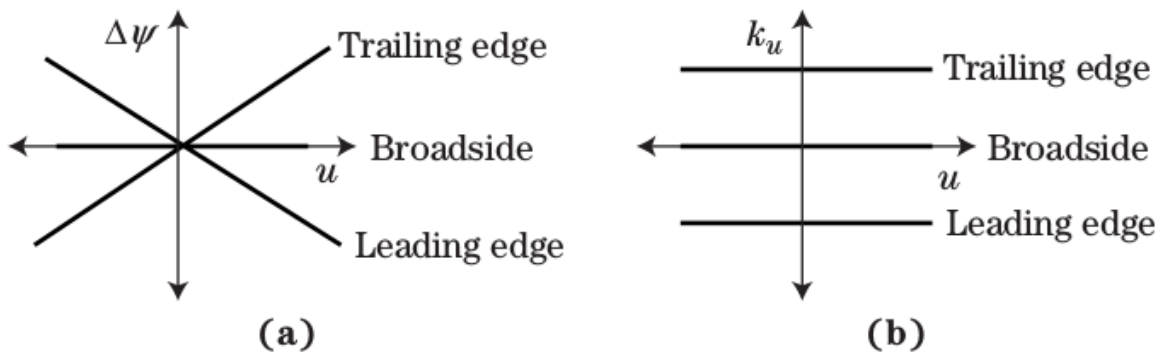

FIGURE 21-22 ■ In the DBS model, (a) phase progressions are approximately linear over the dwell, with slope mapping to cross-range location, and (b) spatial frequencies (Doppler) are approximately constant over the dwell, with frequency mapping to cross-range location.

Doppler Beam Sharpening (DBS) image formation

Fourier transform in platform position (slow time)

$$D(k_u, t) = \int_{-\infty}^{\infty} d(u, t) \mathrm{e}^{-\mathrm{j}k_u u}\, \mathrm{d}u$$

Coordinate mappings:

$$t = \frac{2R}{c} = \frac{2\sqrt{x^2 + r^2}}{c} \approx \frac{2}{c} r$$

$$k_u = -\frac{4\pi}{\lambda_\mathrm{c}} \frac{x}{r} \approx -\frac{4\pi}{\lambda_\mathrm{c}} \frac{x}{r_0}$$

Rescale coordinates to find final image:

$$f(x, r) = D\left[k_u\left(-\frac{\lambda_\mathrm{c} r_0}{4\pi}\right) \to x, t\left(\frac{c}{2}\right) \to r\right]$$

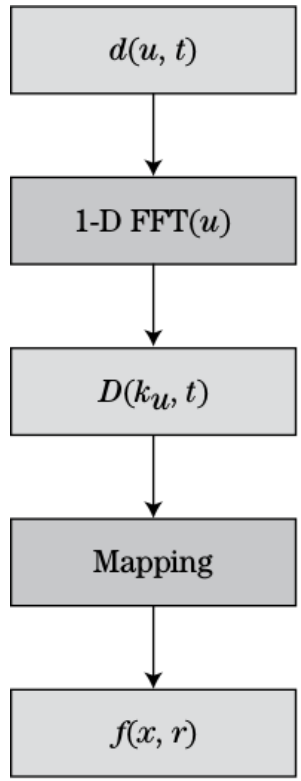

FIGURE 21-23 ■
DBS processing performs a spatial Fourier transform over the pulse history followed by mapping the data into scene coordinates.

DBS example 1

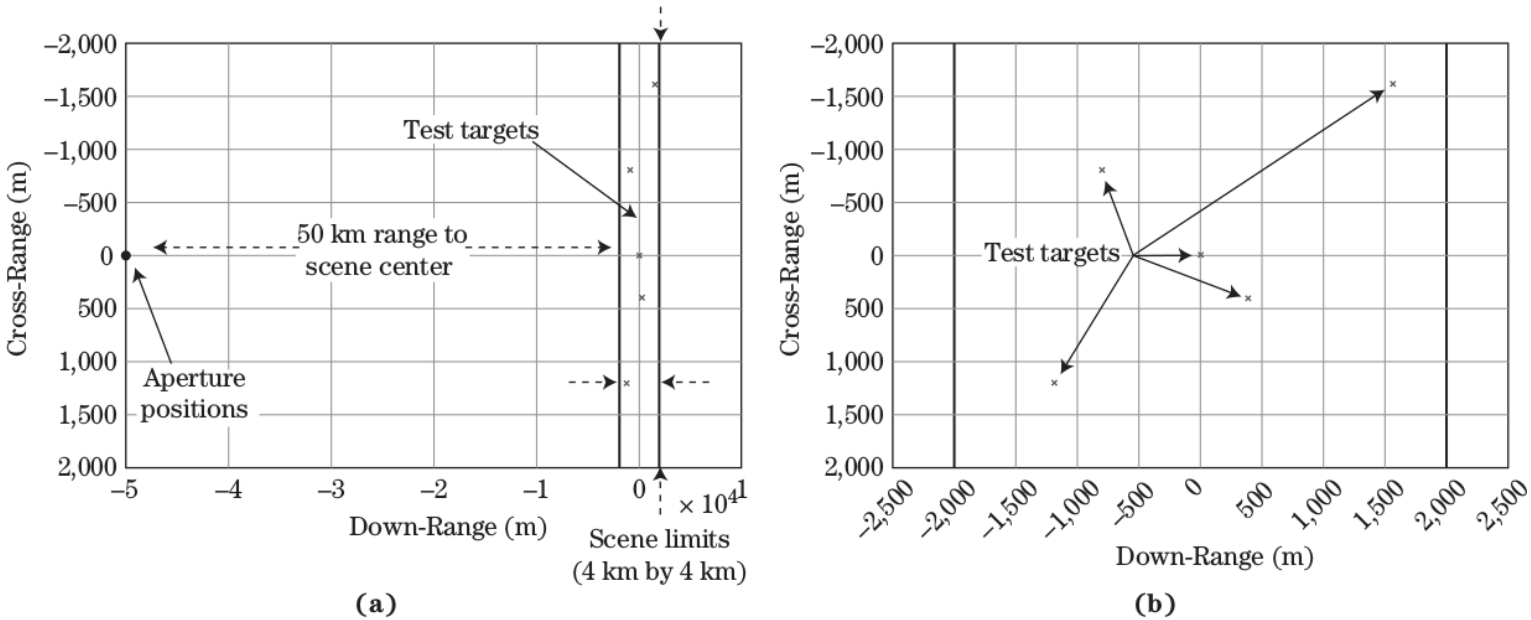

FIGURE 21-24 ■ Simulated DBS geometry emphasizes (a) the overall collection geometry, and (b) point scatterer locations in the scene of interest.

- Carrier frequency = 9.6 GHz.
- RF bandwidth = 3 MHz.
- Integration angle = 0.02°.
- Resolution = 50 m (both dimensions).
- Number of along-track sample points (pulses) = 80.
- Range to scene center = 50 km.

DBS example 1: raw data, absolute value

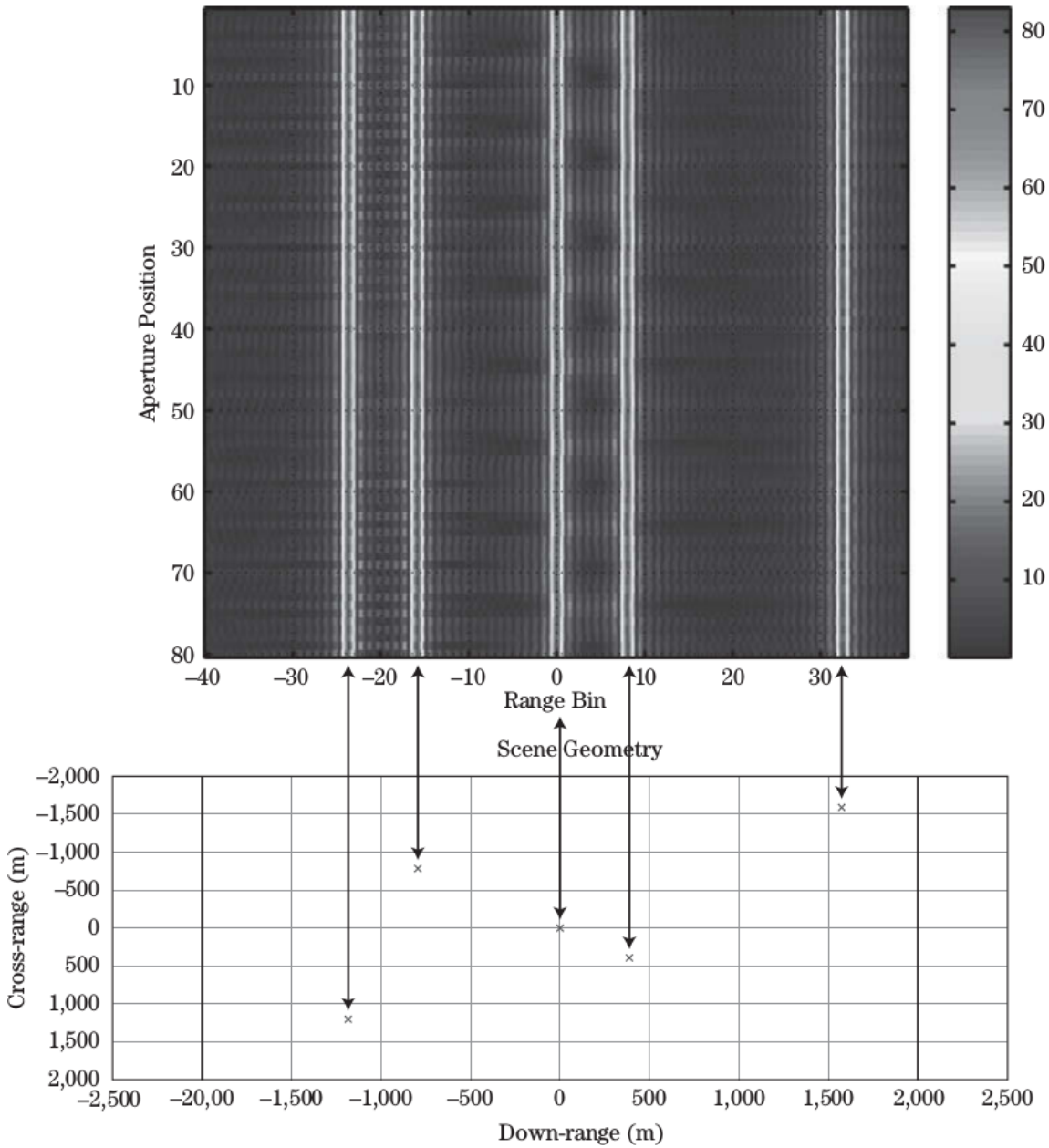

FIGURE 21-25 ■ Mapping of HRR profiles in the raw data to scatterer locations in the scene of interest.

DBS example 1: raw data, real part

FIGURE 21-26 ■
Real part of the HRR profiles, with positive voltages in white and negative voltages in black, indicates phase changes over the dwell and, therefore, Doppler frequency.

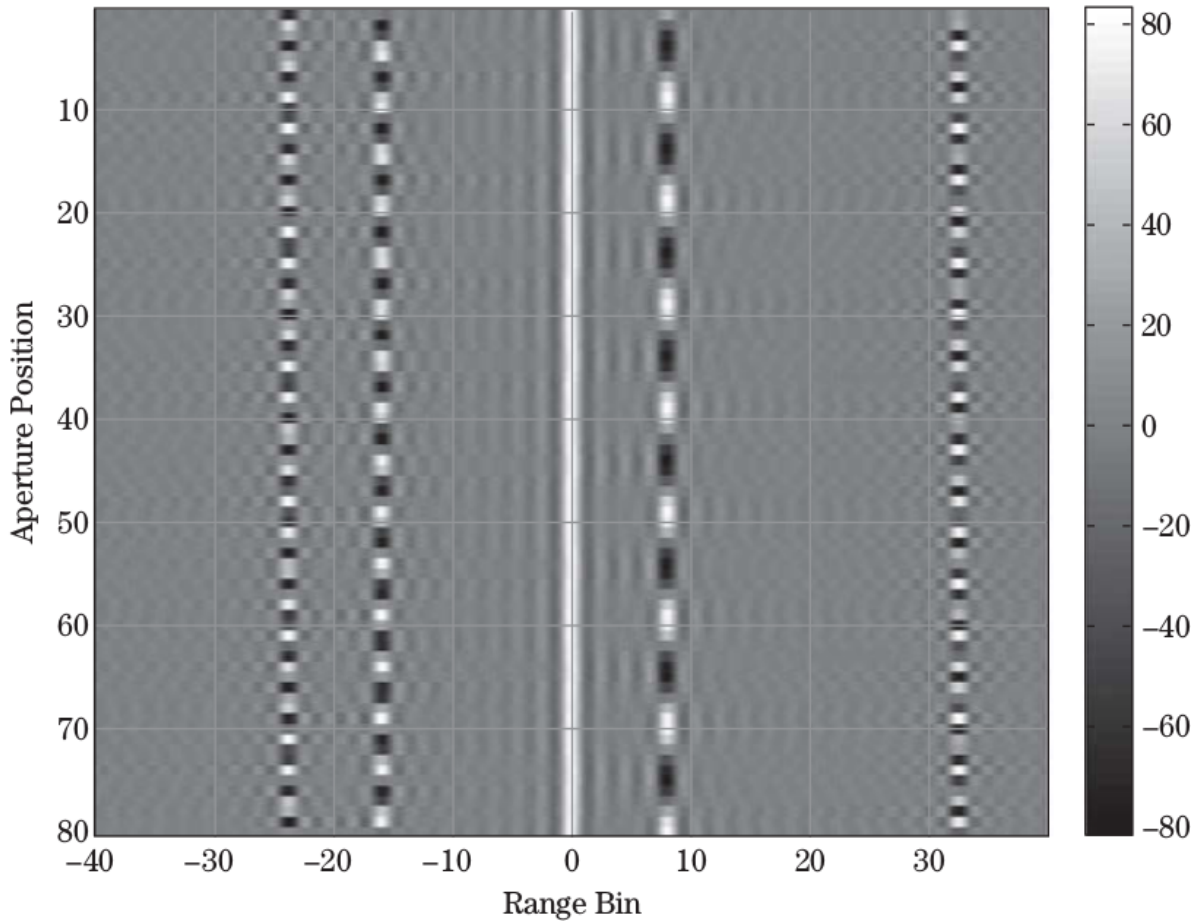

Phase shifts due to different cross-range positions of the targets.

DBS example 1: processed data

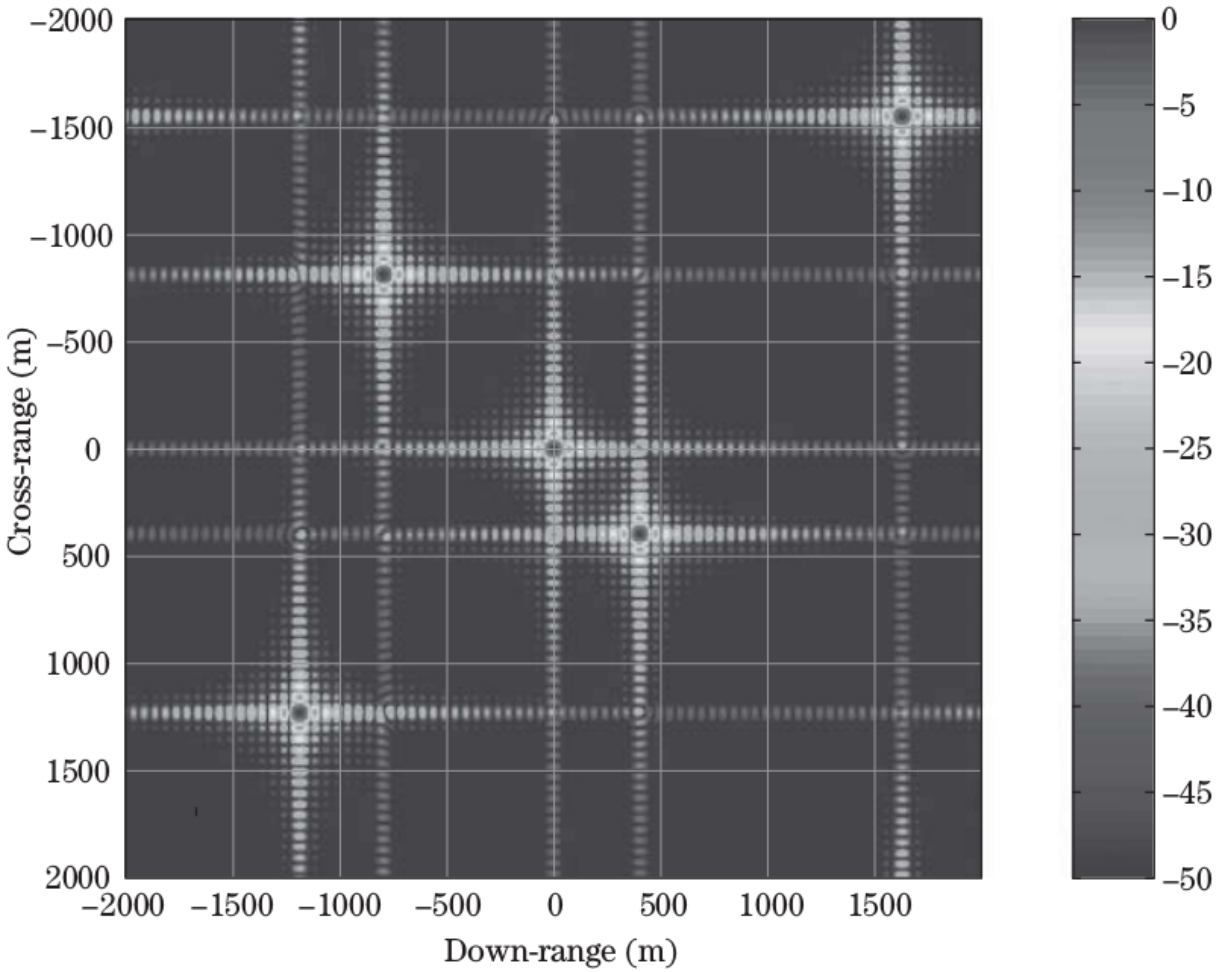

FIGURE 21-27 ■ DBS image of the simulated point targets.

The crosses correspond to two-dimensional sinc functions, typical from Fourier transformations of rectangular pulses. Can be suppressed by windowing, at the cost of reduced resolution.

DBS example 2: challenging the algorithm

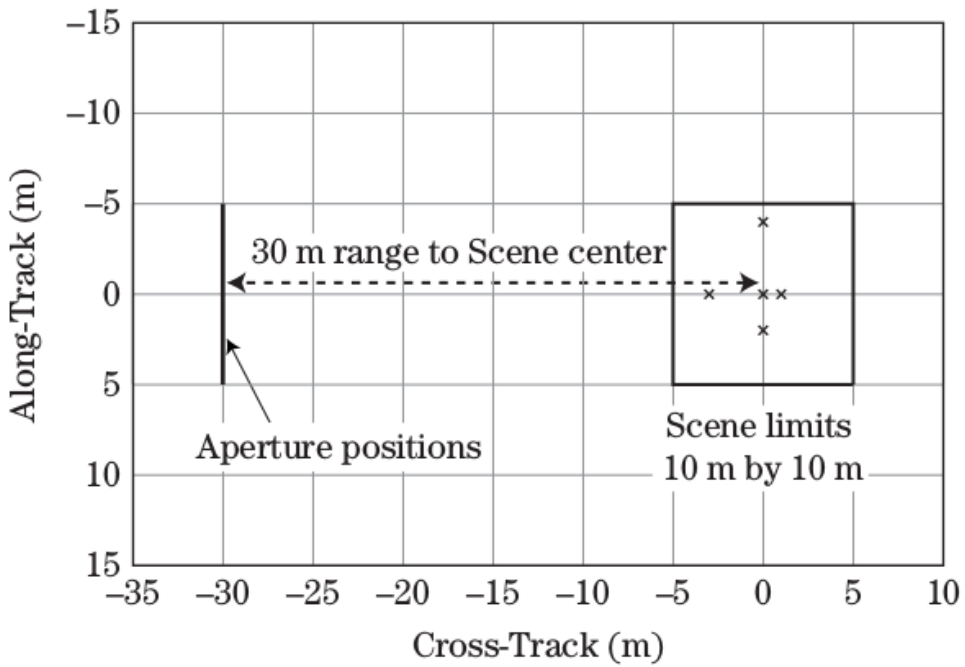

FIGURE 21-28 ■
A challenging, near-range collection geometry.

- Carrier frequency = 3 GHz.
- Integration angle = 51°.
- Resolution = 0.2 m (both dimensions).
- Number of along-track sample points (pulses) = 275.
- Range to scene center = 30 m.

▸ Discussion

DBS example 2: raw data, real part

FIGURE 21-29 ■
Real part of the HRR profiles for the near-range collection. Tremendous range migration and higher-order phase modulations are apparent in the raw data.

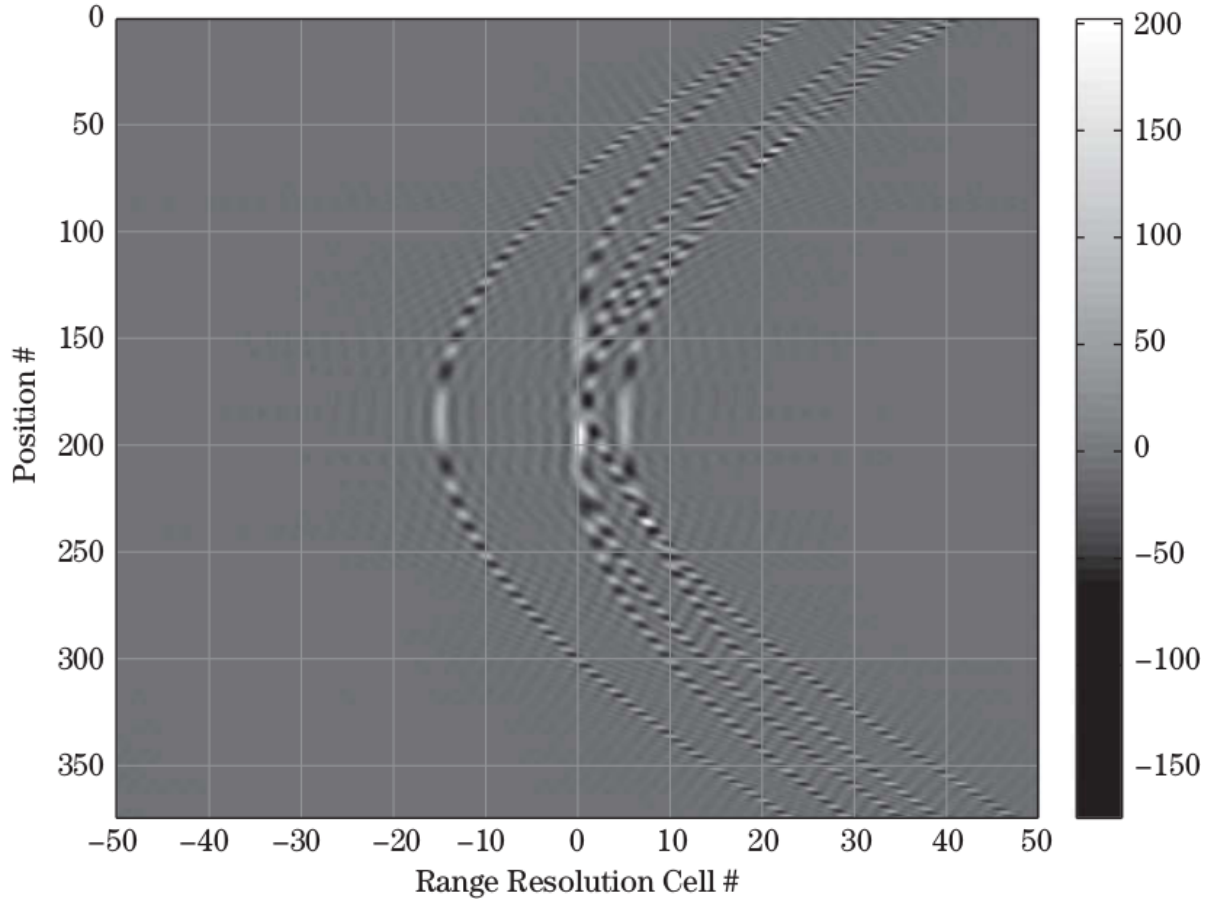

Significant range migration and higher order phase modulation.

DBS example 2: processed data

FIGURE 21-30 ■
The DBS image of the near-range point targets is distorted and unusable.

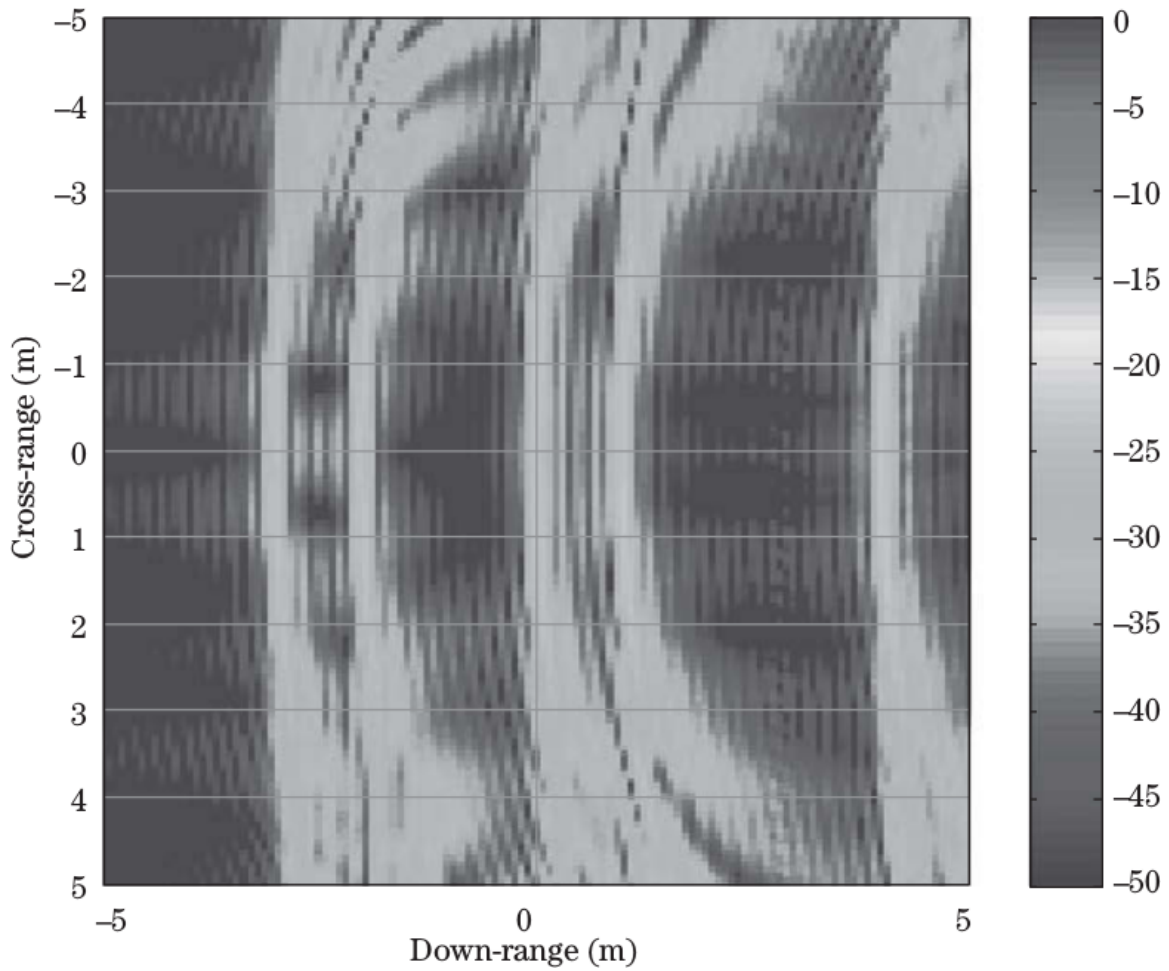

Standard DBS processing does not produce a useful image.

Matched filter imaging

More sophisticated imaging methods are necessary when the assumptions of the DBS are not valid. A reference signal d_{REF} is defined by the PSR

$$t(u;x,r) = \frac{2}{c}\sqrt{(u-x)^2+r^2} \quad \Rightarrow \quad d_{\mathrm{REF}}(u,t;x,r) = \delta_{\mathrm{D}}(t - t(u;x,r))$$

The image can then be computed from the matched filter approach

$$f(x,r) = \int_{-\infty}^{\infty}\int_{-\infty}^{\infty} d(u,t) d^{*}_{\mathrm{REF}}(u,t;x,r)\,\mathrm{d}u\,\mathrm{d}t$$

which reduces to the (time-domain) back-projection algorithm

$$f(x,r) = \int_{-\infty}^{\infty} d(u,t(u;x,r))\,\mathrm{d}u$$

This usually entails resampling and interpolating the data to fit the discretized image coordinates (x,r). Computationally intensive, but less geometry dependent than DBS.

Example 2: matched filter result

FIGURE 21-31 ■
Matched filter image of the near-range point targets is accurate.

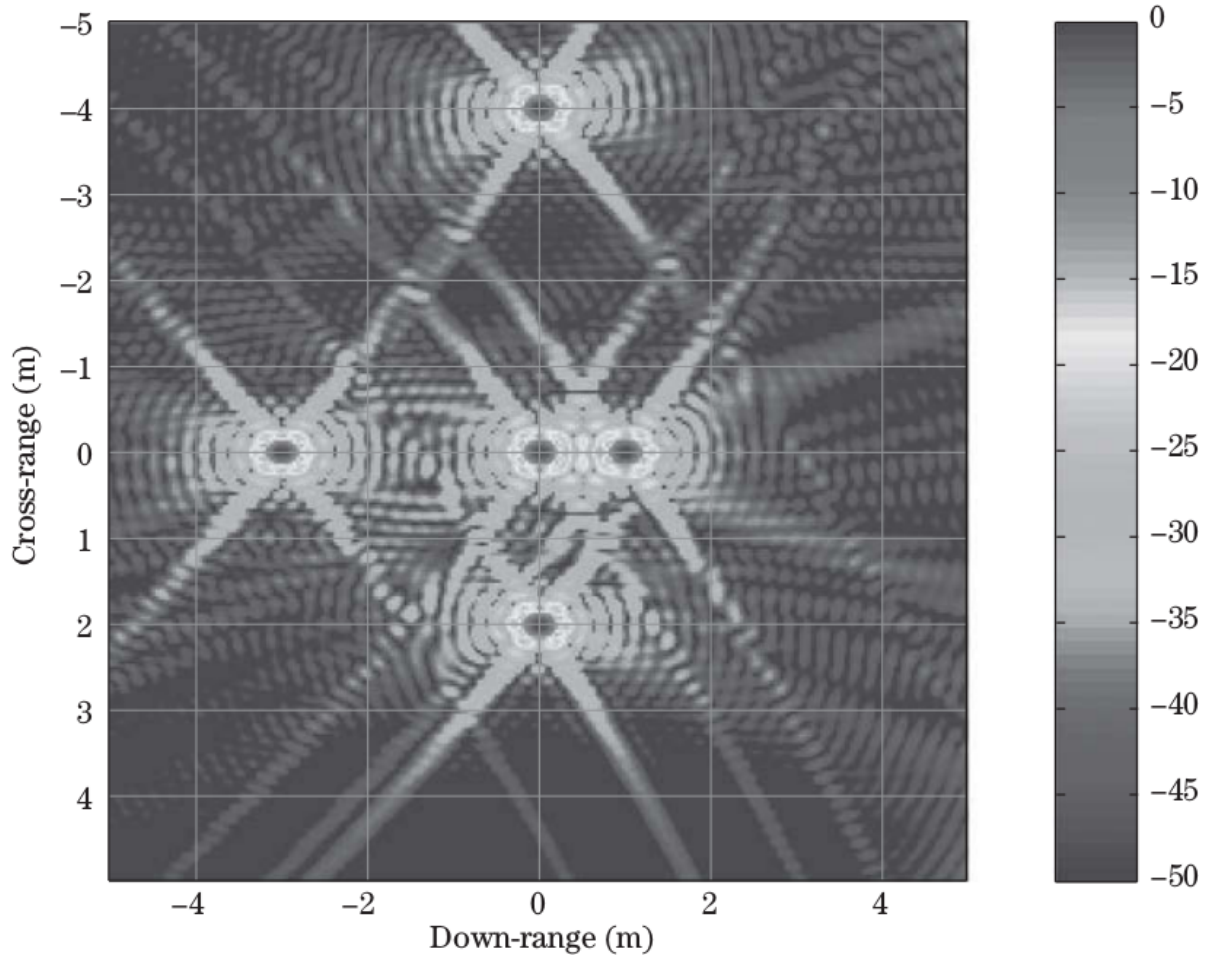

The constraints of the DBS assumptions are relaxed.

Image formation survey

TABLE 21-1 ■ Survey of SAR Image Formation Algorithms

Category	Features	Limitations	Algorithms	Notes
Doppler	Requires only a 1-D FFT after pulse compression	No accounting for migration of scatterers through range bins or phase orders above linear	Doppler beam sharpening	Fourier transform provides the "matched filter"
			DBS with azimuth dechirp	Accounts for QPE by applying a conjugate quadratic modulation to the data prior to DBS
Fourier Matched Filter	Match filtering with the PSR implemented efficiently by multiplication in the frequency domain	Data acquisition must be linear with uniform spacing between along-track samples	Range-Doppler algorithm	Assumes a single PSR is good for the entire scene, so focused swath depth is limited
			Range migration algorithm	Range Doppler algorithm combined with Stolt data interpolation provides error-free imaging over deep swaths
			Chirp scaling algorithm	Exploits direct sampling of linear FM waveforms to realize a computationally efficient approximation to the Stolt interpolation
			Range stacking algorithm	Like RMA, but less computationally efficient
Tomographic	Projection-slice view of data acquisition; efficient image formation follows	Scene size; data must be time delayed and phase corrected prior to image formation	Rectangular formatting algorithm	Analogous to DBS in simplicity; capable of fine resolution, but scene size severely restricted
			Polar formatting algorithm	2-D data interpolation provides quality imaging at fine resolutions over reasonable scene sizes; scene extents ultimately limited by geometric considerations
Inverse	A more holistic, mathematical view of data acquisition and image formation	Demanding processing requirements, and sometimes memory requirements as well	Matched filtering	Employs a product of the data and a reference response; implementable in either time-distance or frequency domains
			Constant aperture backprojection	Delay and sum imaging; same data records used for all pixels
			Constant integration angle backprojection	Like constant aperture backprojection, but different subset of the overall data applied to each pixel to realize a constant integration angle
			Filtered backprojection	Wideband/wide-angle data is preequalized to improve impulse response in the final image
			Fast backprojection	Family of algorithms that garner computational efficiencies by making minor approximations to basic backprojection
			Quad-tree	Fast backprojection using multiresolution topologies
			Constrained inversion	SAR imaging treated as a mathematical inverse problem

Outline

No return areas (NRA): shadows

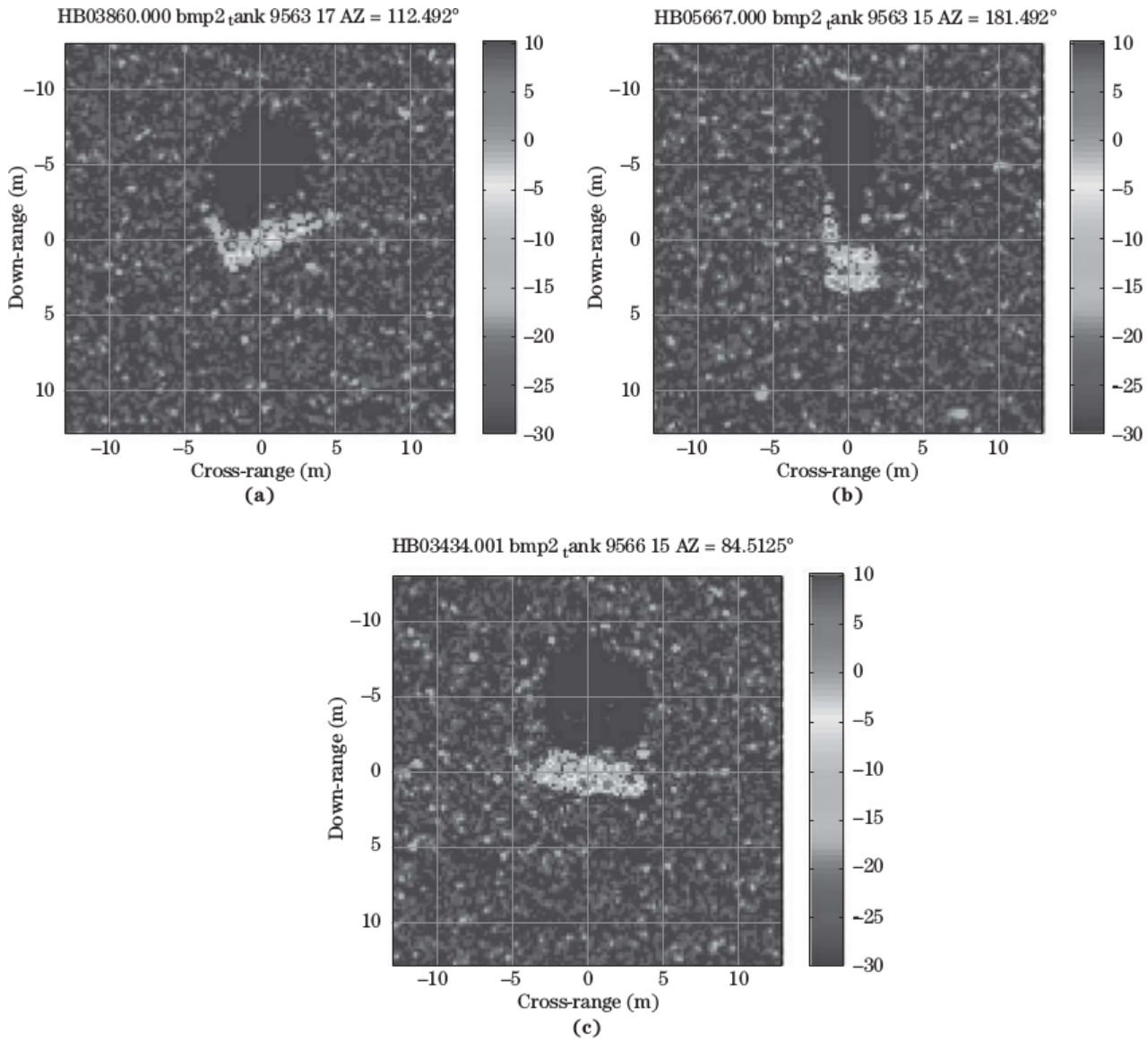

FIGURE 21-32 ■ Three SAR images of an armored vehicle with radar at the bottom of each image and the vehicle (a) at a non-cardinal pose angle, (b) broadside to the radar, and (c) end-on to the radar.

Paved areas, clutter, man-made objects

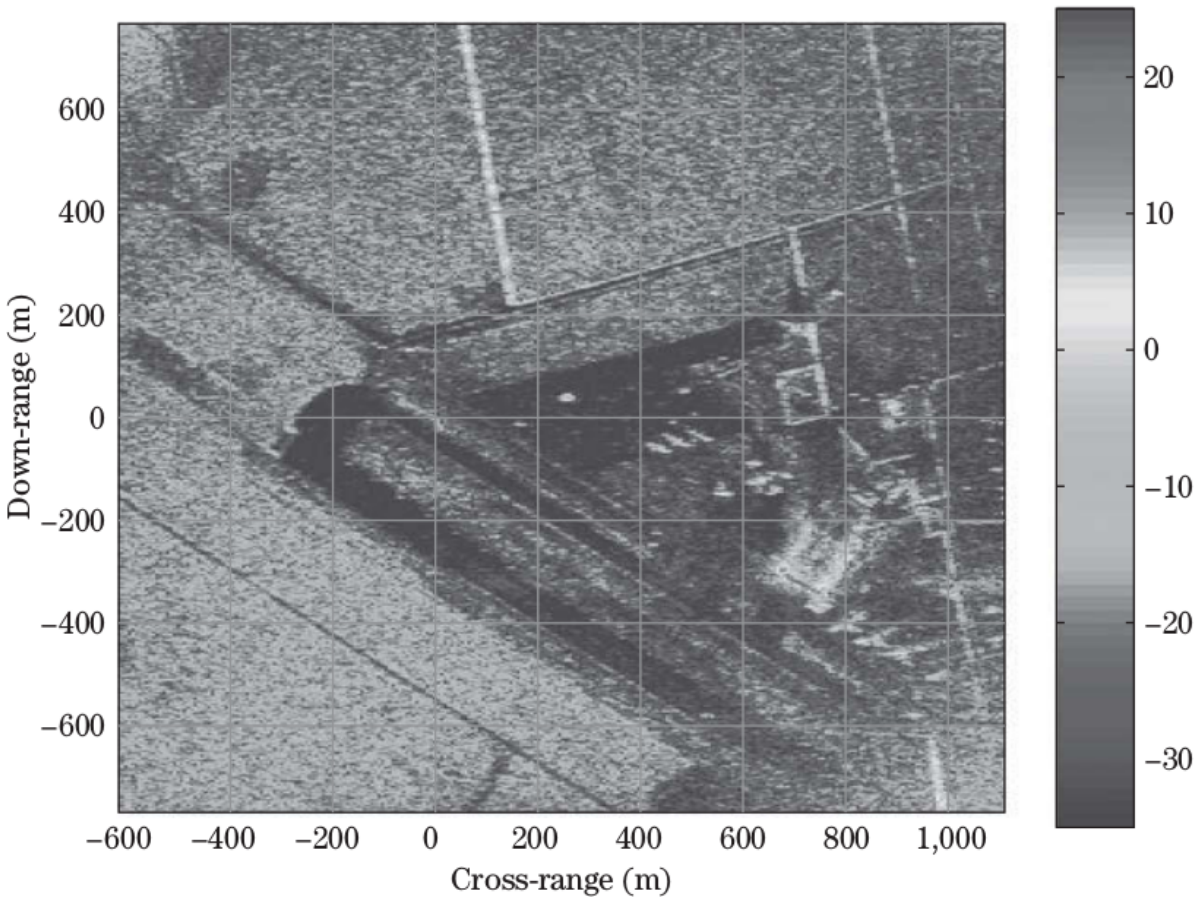

FIGURE 21-33 ■ SAR image of the Mojave Airport showing low-power areas corresponding to runways and tarmac, moderate-power areas off the runways due to natural clutter return, and strong man-made returns near the tarmac. (Data courtesy of Raytheon Corporation.)

Lakes

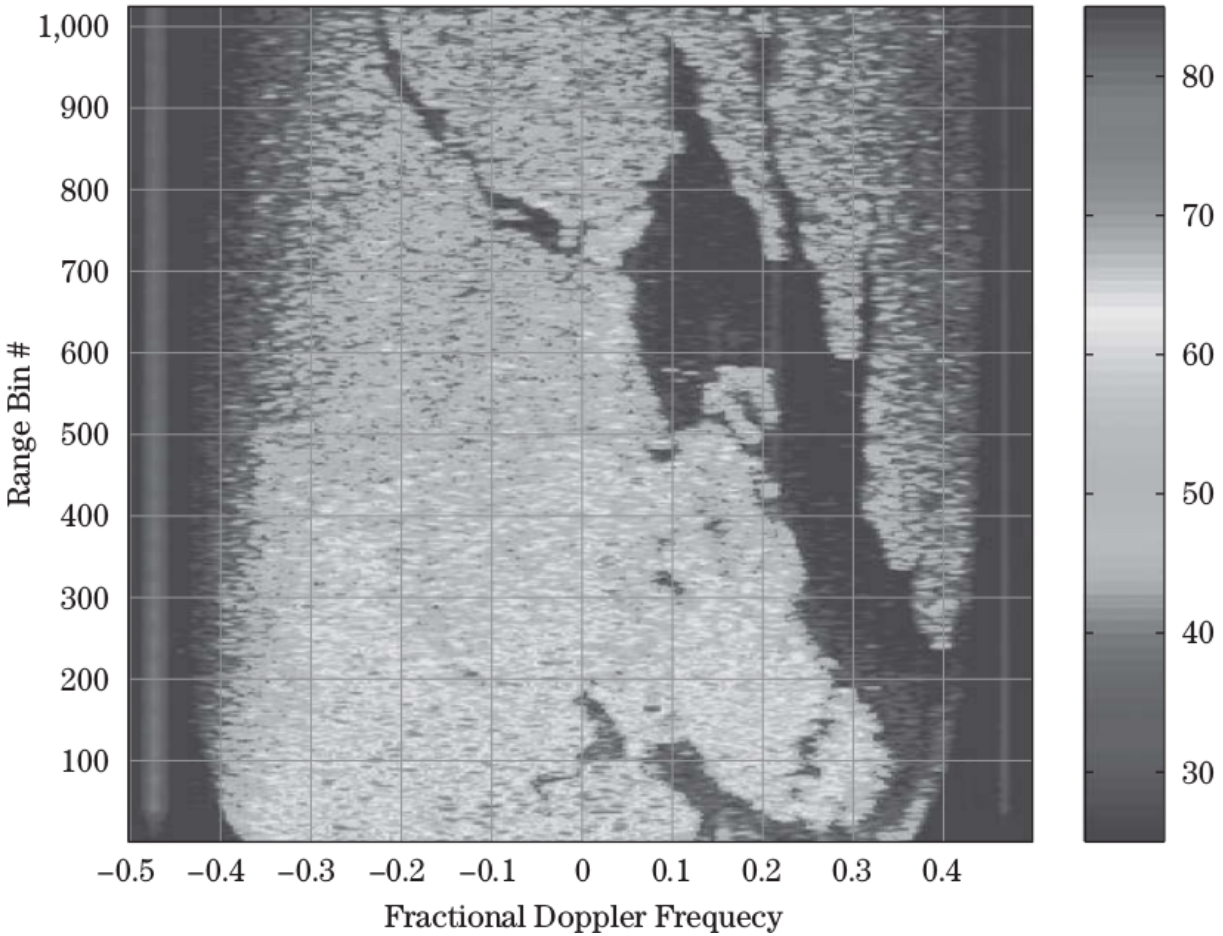

FIGURE 21-34 ■ Coarse-resolution DBS image emphasizing the contrast in power between land and water regions. (Data courtesy of Northrop Grumman Corporation.)

Still water has specular scattering, producing very little return.

Shadow, fore-shortening

FIGURE 21-35 ■
Foreshortening: Targets having great height will appear collapsed in a SAR imaged collected with a significant grazing angle.

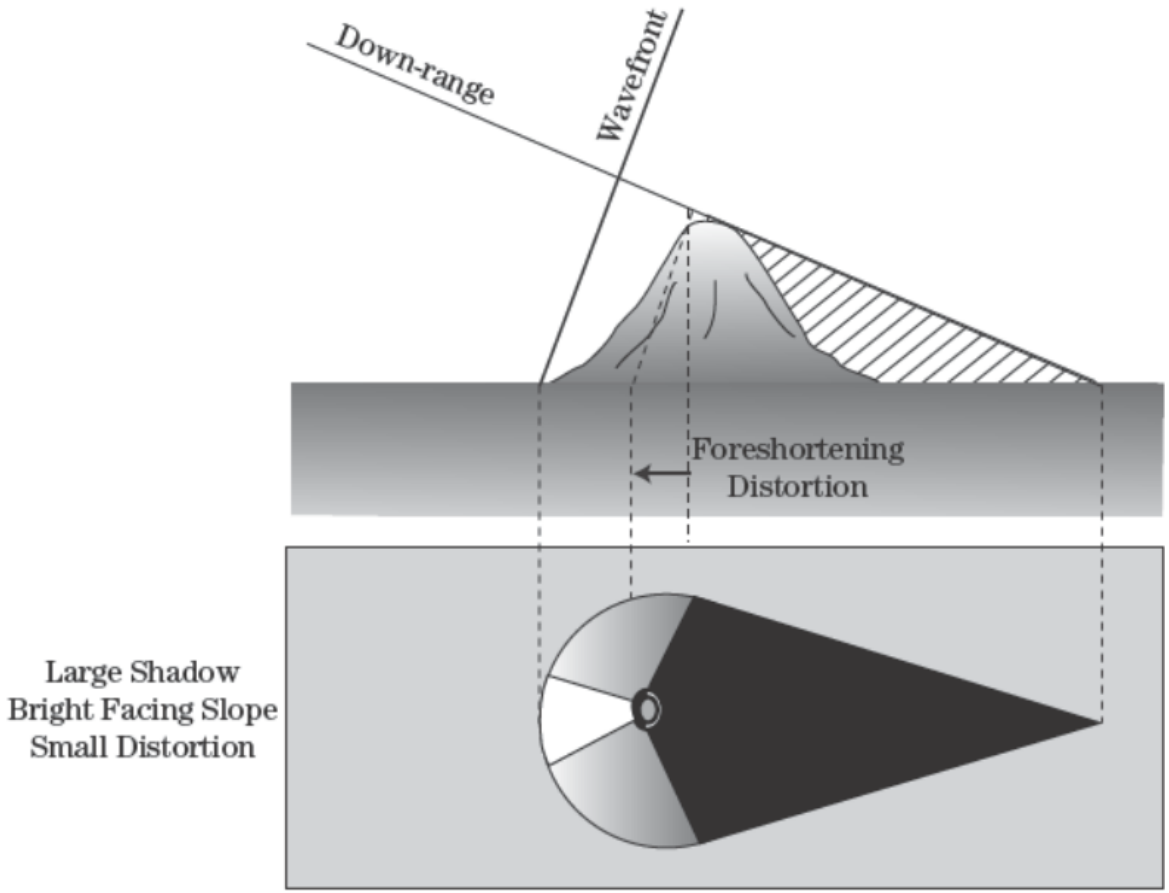

Shadow shapes provide information on target shapes. The increased slope of the terrain makes a stronger return than flat ground, causing a combination of bright and dark spots. Fore-shortening is the range compression of the illuminated hill.

Layover

FIGURE 21-36 ■
Layover: In collections having steep lookdown angles and significant height variations, scatterer order may appear reversed in the down-range direction.

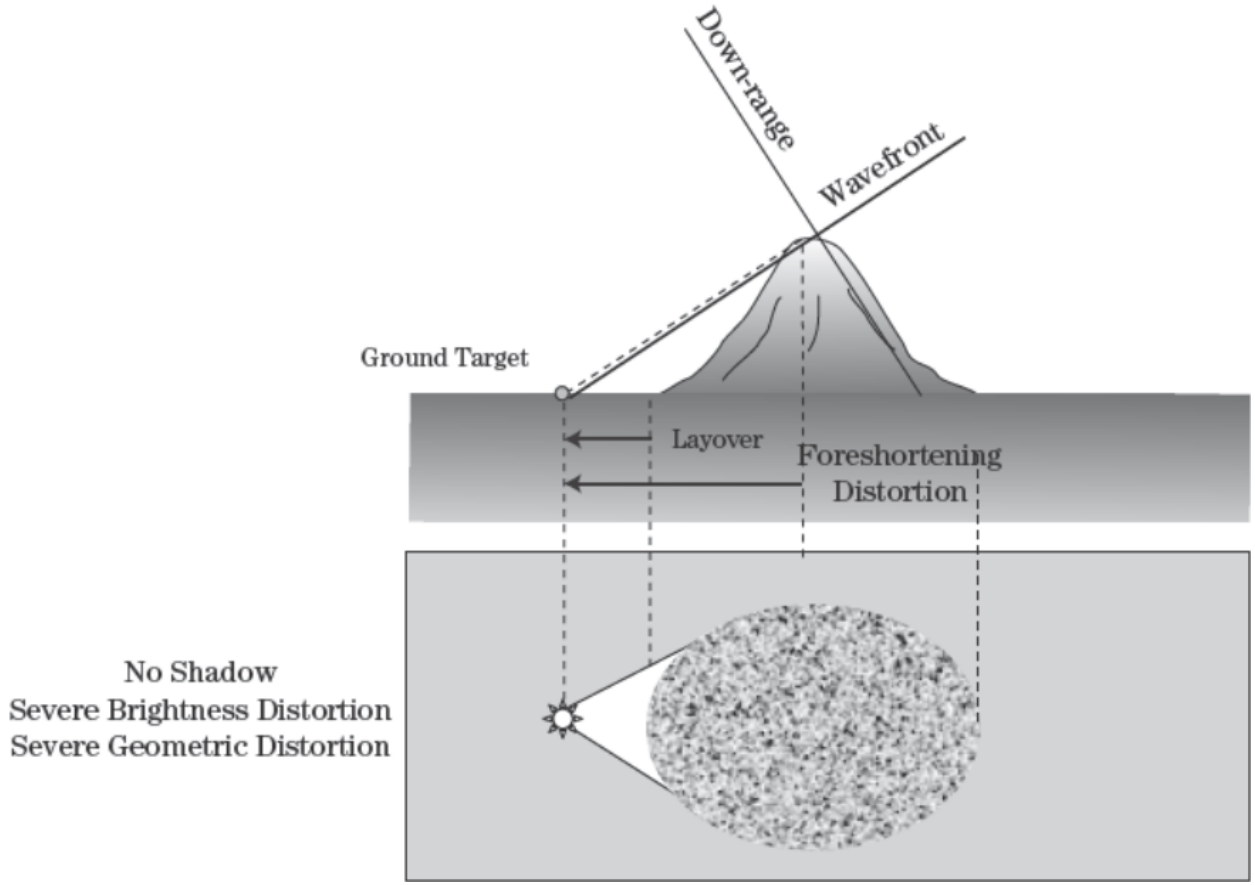

Steep angles cause tall objects to appear earlier in the image than the expected ground return. Some effects can be studied at http://www.nrcan.gc.ca/node/9325.

▸ Discussion

Speckle

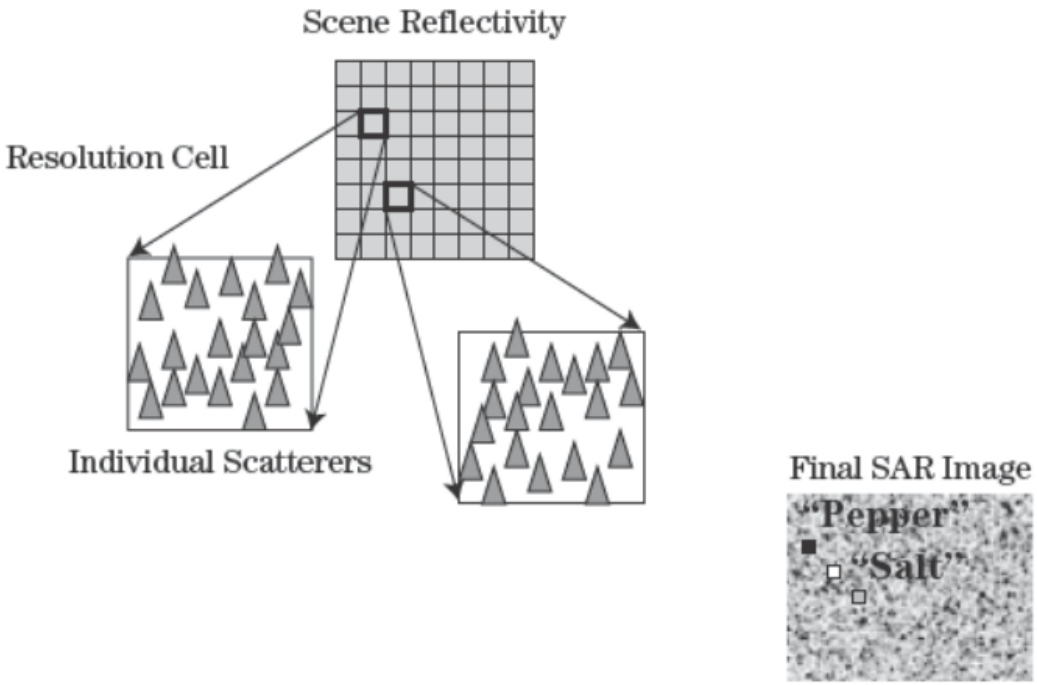

FIGURE 21-37 ■ Speckle is the natural consequence of coherent imaging on a scene having a large number of small, unresolved, randomly placed scatterers.

Constructive and destructive interference from many scatterers produce a speckled pattern, varying from pixel to pixel.

Speckle reduction by multilook and averaging

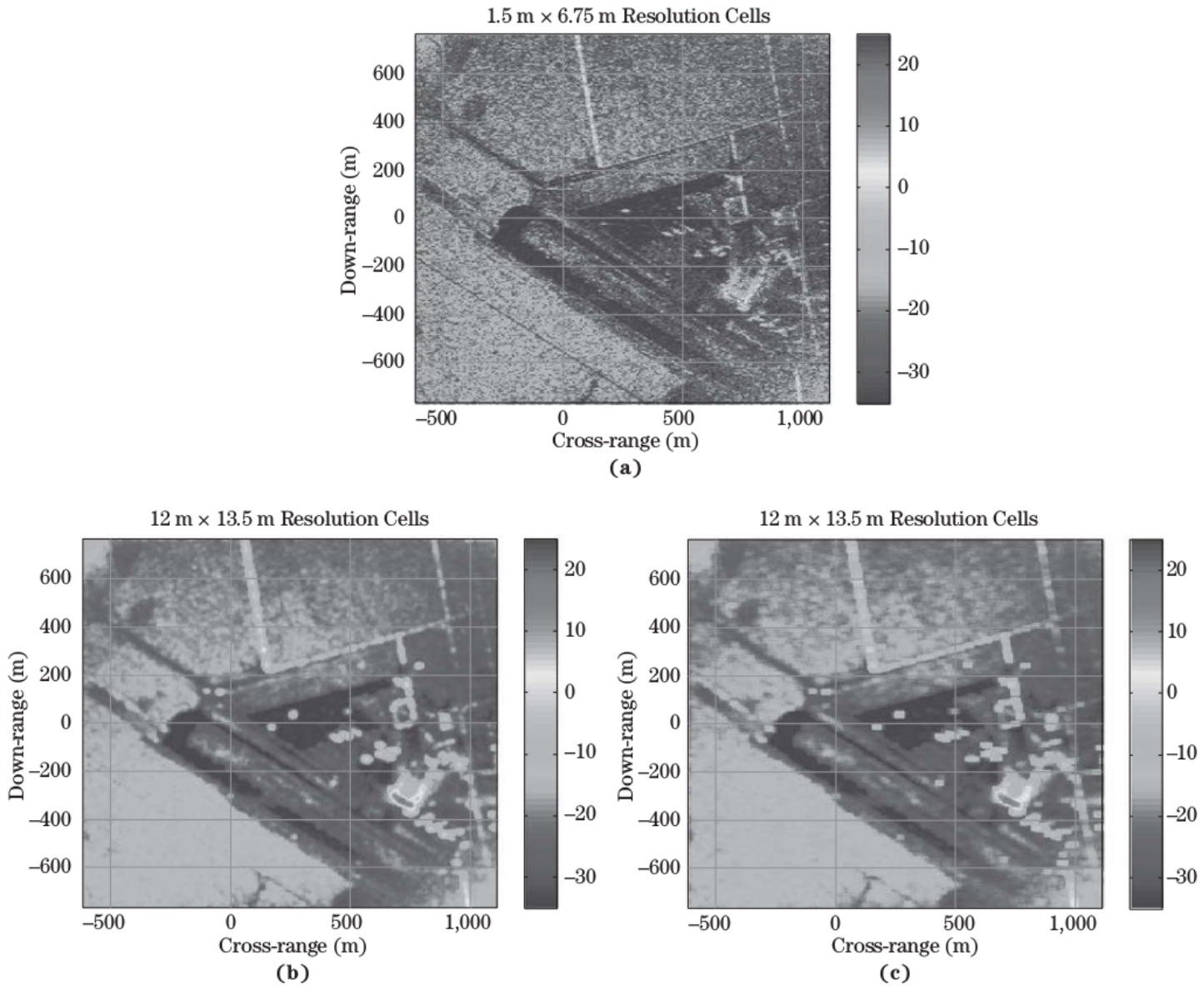

FIGURE 21-38 ■ Speckle reduction on (a) the original image using (b) multi-look processing and (c) image-domain filtering. (Data courtesy of Raytheon Corporation.)

Man-made returns

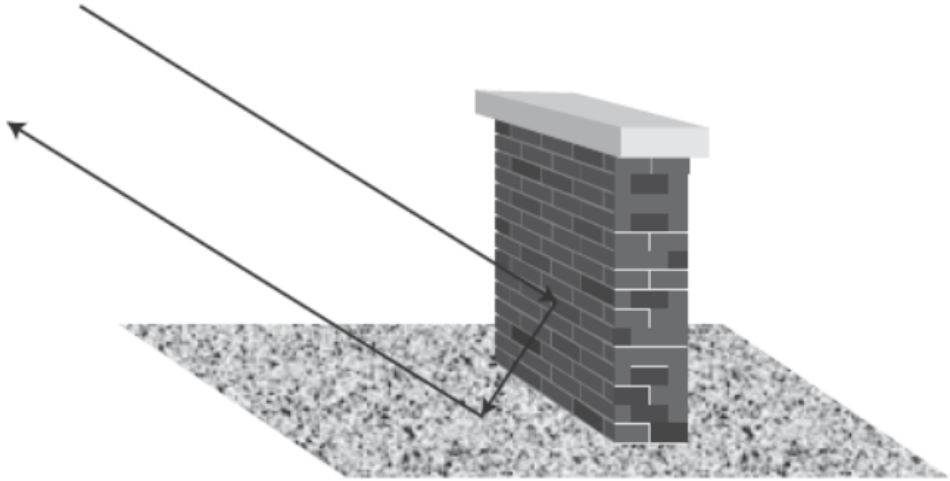

FIGURE 21-39 ■
Geometry for two-plane retro-reflection.

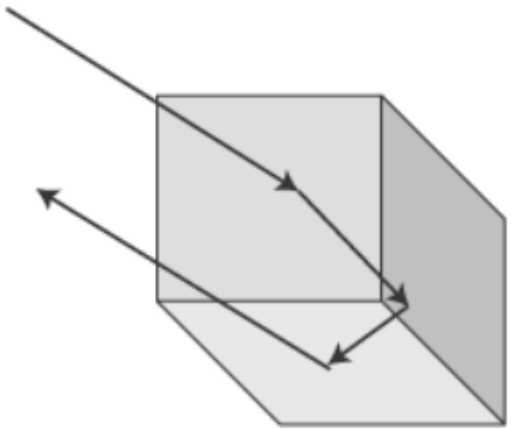

FIGURE 21-40 ■
Geometry for three-plane retro-reflection.

Man-made objects tend to have significant structure and finite extent, as compared to lawns, fields, forests etc. Typically metal structures, smooth surfaces, and right-angle corners, can cause strong reflections.

Man-made returns

FIGURE 21-41 ■ Armored vehicle presents a complicated and faceted surface (see images in Figure 21-32).

Strong returns from the dihedral formed by ground and flat side. Several minor features in the vehicle may cause retroreflection.

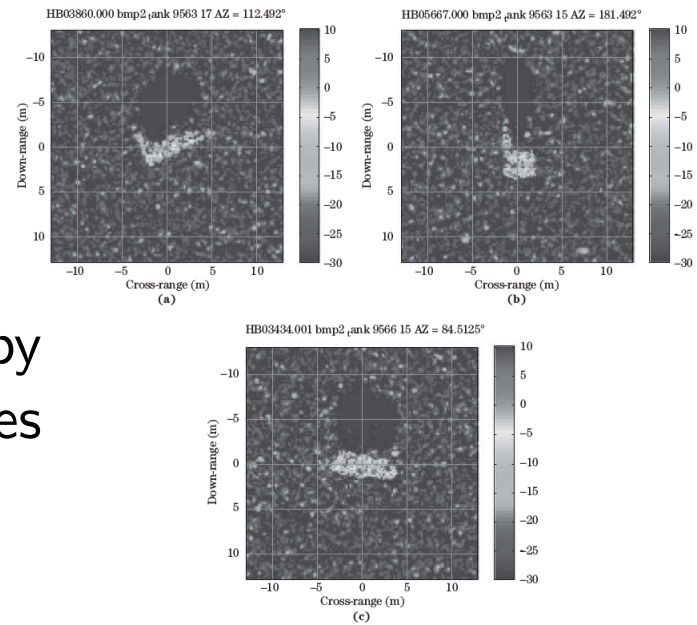

FIGURE 21-32 ■ Three SAR images of an armored vehicle with radar at the bottom of each image and the vehicle (a) at a non-cardinal pose angle, (b) broadside to the radar, and (c) end-on to the radar.

Signal-to-noise and clutter-to-noise ratios

The radar range equation can be rewritten in terms of parameters relevant to SAR imaging.

Signal-to-noise ratio

$$\mathrm{SNR} = \frac{P_{\mathrm{avg}} G_{\mathrm{t}} G_{\mathrm{r}} \lambda^3 \sigma}{2v \sin\theta_{\mathrm{cone}} (4\pi)^3 R^3 N_0 L_{\mathrm{s}} \Delta\mathrm{CR}}$$

Clutter-to-noise ratio ($\sigma_{\mathrm{c}} = \sigma^0 A_{\mathrm{c}} = \sigma^0 \Delta\mathrm{CR} \Delta R / \cos\delta$)

$$\mathrm{CNR} = \frac{P_{\mathrm{avg}} G_{\mathrm{t}} G_{\mathrm{r}} \lambda^3 \sigma^0 \Delta R}{2v \sin\theta_{\mathrm{cone}} \cos\delta (4\pi)^3 R^3 N_0 L_{\mathrm{s}}}$$

Noise-equivalent backscatter coefficient (σ^0 for which $\mathrm{CNR} = 1$)

$$\sigma_n = \frac{2v \sin\theta_{\mathrm{cone}} \cos\delta (4\pi)^3 R^3 N_0 L_{\mathrm{s}}}{P_{\mathrm{avg}} G_{\mathrm{t}} G_{\mathrm{r}} \lambda^3 \Delta R}$$

This limits the possible contrast between different terrain types.

Outline

Conclusions

- Radar images can be formed using synthetic aperture.
- Down-range resolution from pulse bandwidth, typically using pulse compression of chirped pulses.
- Cross-range resolution from along-track sampling.
- DBS algorithm suitable for long ranges compared to D_{SAR}, uses Fourier transform in cross-range.
- Matched filter or backprojection is more computationally demanding, but relaxes geometry constraints.
- Radar images tend to emphasize returns from man-made objects.

Discussion

With Doppler resolution $\Delta f_{\mathrm{d}} = 1/T_{\mathrm{d}}$ and $f_{\mathrm{d}} = 2v\cos\theta/\lambda$, how would you compute the angle resolution $\Delta\theta$?

◂ Go back

Discussion

With Doppler resolution $\Delta f_\mathrm{d} = 1/T_\mathrm{d}$ and $f_\mathrm{d} = 2v\cos\theta/\lambda$, how would you compute the angle resolution $\Delta\theta$?

Answer: $\Delta\theta \approx \left|\frac{\partial\theta}{\partial f_\mathrm{d}}\right| \Delta f_\mathrm{d} = \left|\frac{1}{\partial f_\mathrm{d}/\partial\theta}\right| \Delta f_\mathrm{d} = \frac{\lambda}{2v\sin\theta}\frac{1}{T_\mathrm{d}} = \frac{\lambda}{2D_\mathrm{SAR}\sin\theta}$, where $D_\mathrm{SAR} = vT_\mathrm{d}$.

◂ Go back

Discussion

FIGURE 21-11 ■ Geometry of overhead photography of a scene of interest as compared to a typical SAR collection.

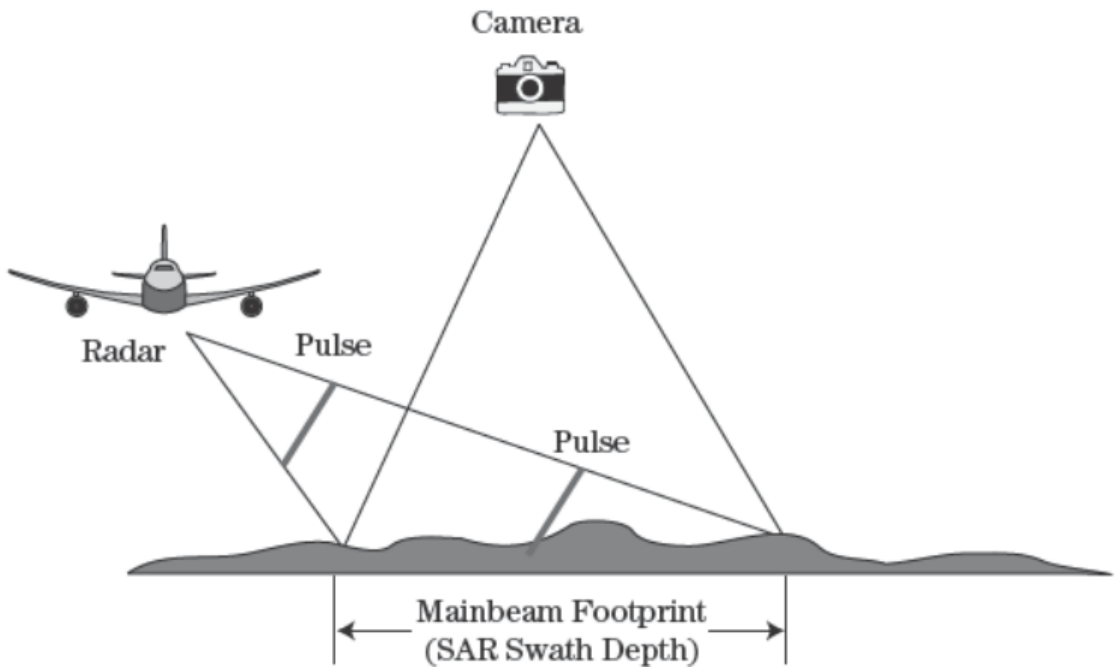

A radar sensor is typically side-looking instead of overhead-looking. Why?

◂ Go back

Discussion

FIGURE 21-11 ■ Geometry of overhead photography of a scene of interest as compared to a typical SAR collection.

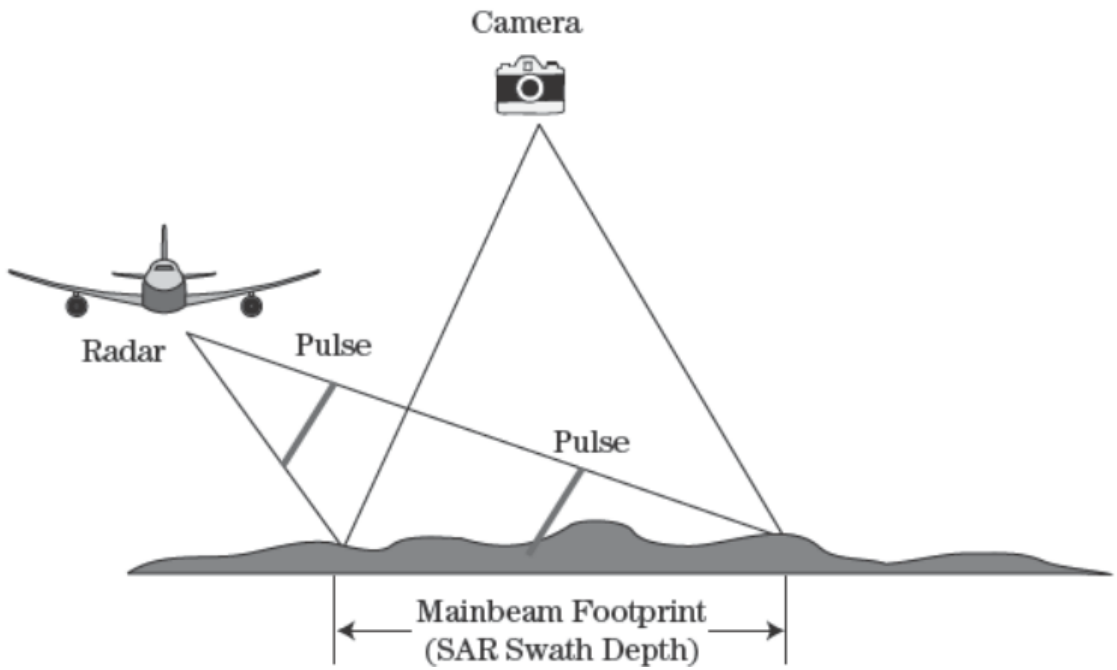

A radar sensor is typically side-looking instead of overhead-looking. Why?

Answer: In the overhead-looking scenario, most of the down-range data end up in the same range bins. Looking sideways, the down-range is more efficiently used.

◂ Go back

Discussion

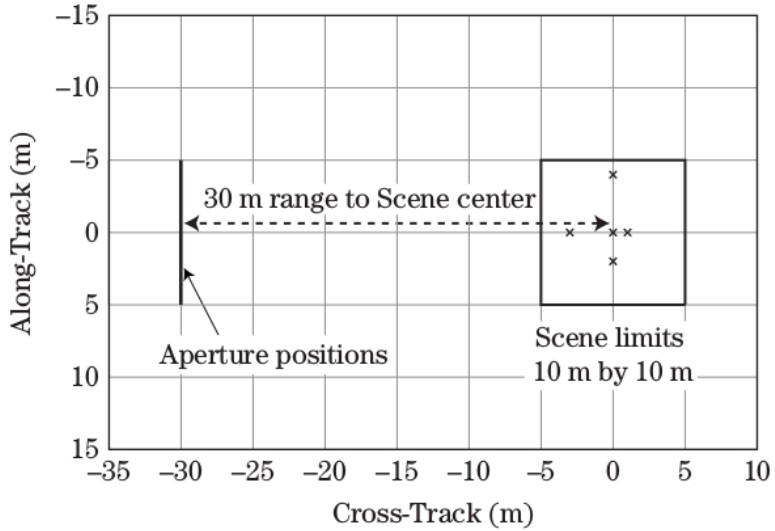

FIGURE 21-28 ■
A challenging, near-range collection geometry.

- Carrier frequency = 3 GHz.
- Integration angle = 51°.
- Resolution = 0.2 m (both dimensions).
- Number of along-track sample points (pulses) = 275.
- Range to scene center = 30 m.

What can be seen as challenging in this scenario?

Discussion

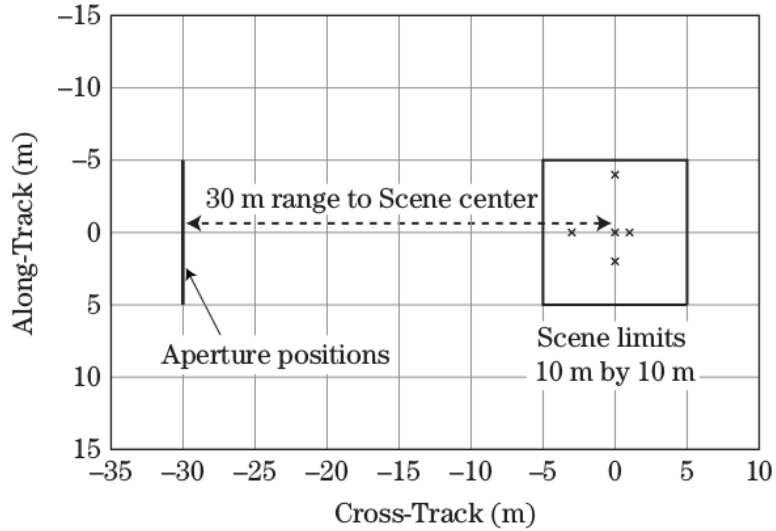

FIGURE 21-28 ■
A challenging, near-range collection geometry.

- Carrier frequency = 3 GHz.
- Integration angle = 51°.
- Resolution = 0.2 m (both dimensions).
- Number of along-track sample points (pulses) = 275.
- Range to scene center = 30 m.

What can be seen as challenging in this scenario?

Answer: Large scene compared to range, large RF bandwidth, wide integration angles, fine resolution. Breaking the assumptions of DBS.

Discussion

FIGURE 21-35 ■ Foreshortening: Targets having great height will appear collapsed in a SAR imaged collected with a significant grazing angle.

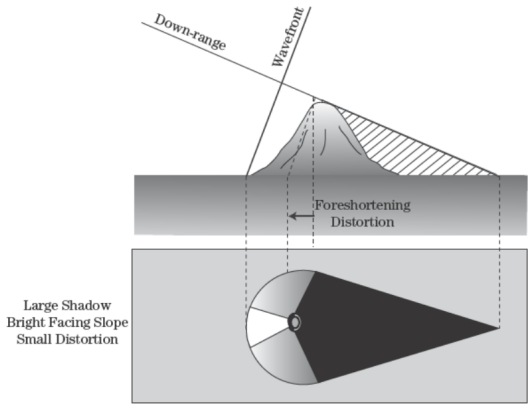

Fore-shortening

FIGURE 21-36 ■ Layover: In collections having steep lookdown angles and significant height variations, scatterer order may appear reversed in the down-range direction.

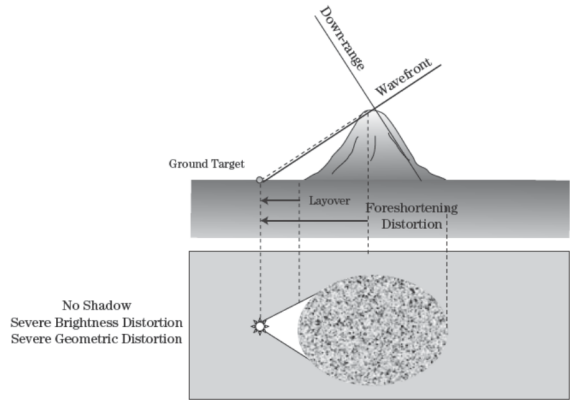

Layover

Which effect tends to make the object larger than it is?

◂ Go back

Discussion

FIGURE 21-35 ■ Foreshortening: Targets having great height will appear collapsed in a SAR imaged collected with a significant grazing angle.

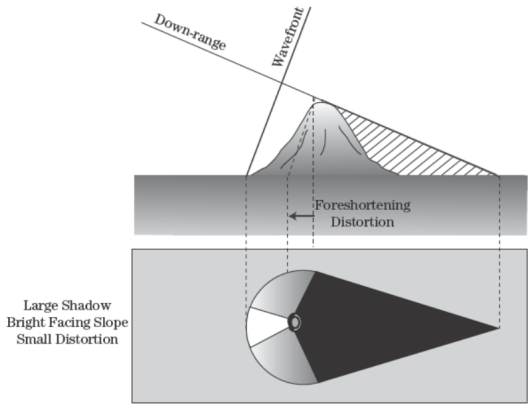

Fore-shortening

FIGURE 21-36 ■ Layover: In collections having steep lookdown angles and significant height variations, scatterer order may appear reversed in the down-range direction.

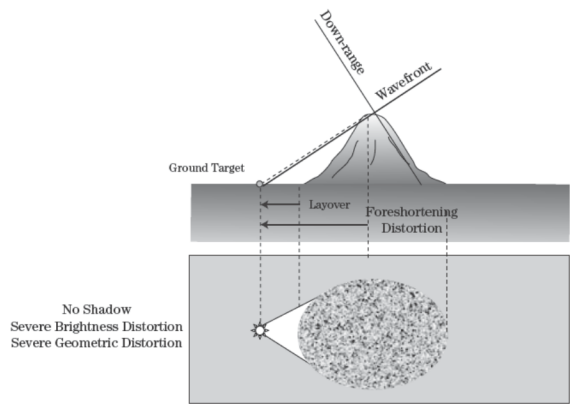

Layover

Which effect tends to make the object larger than it is?

Answer: The layover effect appears as reflections from the ground in front of the object, whereas the fore-shortening makes the peak of the object shift towards the radar but within the object footprint. If there is a shadow, it may cover both part of the object footprint and some distance behind it.

◂ Go back